Reference
NBS
PUBLICATIONS

NAT'L INST. OF STAND & TECH
A11106 228826

NBSIR 84-3013

LASER-INITIATED COMBUSTION STUDIES ON METALLIC ALLOYS IN PRESSURIZED OXYGEN

National Bureau of Standards
U.S. Department of Commerce
Boulder, Colorado 80303

August 1984

QC
100
.U56
No.84-3013
1934

NATIONAL BUREAU
OF STANDARDS
LIBRARY

NBSIR 84-3013

LASER-INITIATED COMBUSTION STUDIES ON METALLIC ALLOYS IN PRESSURIZED OXYGEN

J.W. Bransford

Chemical Engineering Science Division
National Engineering Laboratory
National Bureau of Standards
U.S. Department of Commerce
Boulder, Colorado 80303

August 1984

U.S. DEPARTMENT OF COMMERCE, Malcolm Baldrige, Secretary

NATIONAL BUREAU OF STANDARDS, Ernest Ambler, Director

CONTENTS

		Page
I.	INTRODUCTION	1
II.	EXPERIMENTAL	2
	A. Facility Development	2
	1. High Pressure Chamber	2
	2. Surface Temperature Measurement	6
	a. Broadband Pyrometer	8
	b. Narrowband Pyrometer	8
	3. Interior Temperature Measurement	8
	4. Mass Measurement	9
	B. Experiment	10
	1. Materials	10
	2. Specimen Geometry	10
	3. Experimental Arrangement	12
III.	RESULTS	14
	A. Specimen Heating Rate	14
	1. Aluminum Alloys	15
	2. Iron, Nickel, and Cobalt Alloys	18
	B. Ignition and Combustion Test in Atmospheric Flowing Oxygen	21
	1. Aluminum 6061	21
	2. Iron and Nickel Base Alloys	25
	a. Stainless Steel: AISI 302, 304, 304L, 316, 321, and 347	27
	b. 440C Stainless Steel	29
	c. Nickel Based Alloys: UNS N06600, N06625, N07718	29
	d. Monel 400 and K-500	29

CONTENTS (continued)

	Page
C. Ignition and Combustion Test in Pressurized Oxygen	29
1. Aluminum 6061	30
2. Cobalt Based Alloy, Haynes 188	34
3. Iron Based Alloys	37
a. Carbon Steel 1018	37
b. Stainless Steel: AISI 302, 304, 304L, 316, 321, and 347	37
4. Nickel Based Alloys: UNS N06600, N06625, N07718, and N07750	40
IV. SUMMARY AND FUTURE EFFORT	55
V. ACKNOWLEDGMENTS	56
APPENDIX A. Theory of Two-Color Ratio Pyrometry	A-1
APPENDIX B. Data Definitions	B-1

LIST OF FIGURES AND TABLES

Figure Number		Page
1.	High pressure combustion chamber	4
2.	View of combustion chamber in position	5
3.	Polycrystalline sodium chloride window assembly	7
4.	Experimental set-up in combustion chamber	13
5.	Heating rate of an aluminum alloy specimen in atmospheric nitrogen	16
6.	Heating rate of an aluminum alloy specimen in atmospheric air	17
7.	Heating rate of a 300 series stainless steel specimen in atmospheric air	19
8.	Heating rate of a preoxidized 300 series stainless steel specimen in atmospheric air	20
9.	Typical signals for an aluminum 6061 combustion in atmospheric flowing oxygen	23
10.	Expanded results at ignition for aluminum 6061	24
11.	Brightness and mass correlation for an AISI 300 series stainless steel	26
12.	Typical results for an AISI 300 series stainless steel in flowing oxygen	28
13.	Average surface temperatures at ignition for aluminum 6061	31
14.	Temperature at ignition for a 0.5 mm diameter surface area for aluminum 6061	32
15.	Surface temperatures for an aluminum 6061 for ignition on cool-down	33
16.	Average surface temperature at ignition for Haynes 188	35
17.	Average surface temperature at combustion for Haynes 188	36
18.	Interior temperature at ignition for carbon steel 1018	38
19.	Average surface temperature at ignition for carbon steel 1018	39
20.	Interior temperature at ignition for AISI 302	41

LIST OF FIGURES AND TABLES (continued)

Figure Number		Page
21.	Average surface temperature at ignition for AISI 302	42
22.	Interior temperature at combustion for AISI 302	43
23.	Average surface temperature at combustion for AISI 302	44
24.	Interior temperature at ignition for AISI 304	45
25.	Average surface temperature at ignition for AISI 304	46
26.	Average surface temperature at combustion for AISI 304	47
27.	Interior temperature at ignition for AISI 316	48
28.	Average surface temperature at ignition for AISI 316	49
29.	Interior temperature at combustion for AISI 316	50
30.	Average surface temperature at combustion for AISI 316	51
31.	Interior temperature at ignition for UNS N06625	52
32.	Average surface temperature at ignition for UNS N06625	53
33.	Average surface temperature at combustion for UNS N06625	54
B.1.	Expanded view of an aluminum alloy ignition	B-2
B.2.	Average surface temperature history for a test of a 300 series stainless steel	B-3
B.3.	Expanded view of the ignition and combustion sequence for a 300 series stainless steel	B-5

Table Number		
1.	Material composition	11

Laser-Initiated Combustion Studies on Metallic Alloys in Pressurized Oxygen*

James W. Bransford
National Bureau of Standards
Boulder, Colorado 80303

The interim results of ignition and combustion studies on aluminum, cobalt, iron, and nickel based alloys are presented. It was found that aluminum alloys could be ignited below the melting point of the product alloy oxides. It was also found that the cobalt, iron, and nickel based alloys generally ignited slightly below to slightly above the melting range of the respective alloy. Unsupported combustion could not be achieved until the alloys and oxides were in the liquid state.

Key words: alloy; combustion; ignition; metal; oxygen compatibility

*Certain commercial equipment, instruments, and materials are identified in this paper to adequately specify the experimental procedure and materials studied. In no case does such identification imply recommendation or endorsement by the National Bureau of Standards, nor does it imply that the material or equipment identified is necessarily the best available for the purpose.

1. INTRODUCTION

This interim report presents the follow-on work on Government Order H43201B - Combustion of Metals in Oxygen. The initial report[1] on this contract described the results of experiments carried out on small irregular-shaped samples of four aluminum alloys, three stainless steels, and two copper alloys. The experiments provided qualitative information on the ignitability, combustibility, and brightness profile, and quantitative data on combustion temperatures and oxygen consumption rate. From the oxygen consumption rate, brightness, and photographic data, several conclusions about the ability to obtain an ignition point (Appendix B), using the laser heating technique, were arrived at. These were:

1. For vapor burning materials - aluminum and aluminum alloys, titanium and titanium alloys, for example - an ignition point could be readily determined since signal profiles were sharp and unambiguous.
2. For liquid surface burning materials - stainless steels, nickel alloys, for example - the signal profiles had slow rise-times and irregular shapes. Thus, defining an ignition point was expected to be difficult but achievable.

With the establishment of the feasibility of obtaining an ignition point, or at least a point above which ignition was highly probable, the actions required for the follow-on effort were defined. These actions were:

1. Construct a high pressure chamber and obtain support equipment.
2. Develop an adequate flameproof lining for the chamber.
3. Develop interior and exterior high temperature measurement capability.
4. Develop mass measurement capability under pressurized conditions.
5. Establish criteria for defining the ignition point.

[1]Bransford, James W. and Clark, Alan F., NBSIR 81-1647, April 1981.

The above actions have subsequently been carried out and are discussed in the following sections along with the results of measurements made to 6.9 MPa.

II. EXPERIMENTAL

A. Facility Development

The original combustion facility was set-up primarily to study titanium combustion at atmospheric pressure with the sample blanketed by flowing oxygen. A small chamber was available but had very limited viewing; the pressure capability was from vacuum to less than 0.2 MPa. Temperature measuring capability was limited to a radiant intensity pyrometer and to a rapid scanning spectrometer, both of which were inadequate for the fast, precise temperature measurements needed for the high pressure experiments. The pyrometer was adversely affected by smoke and window clouding; the rapid scanning spectrometer was too slow and could not be used for continuous measurements during the experiment. Mass measurements were made on an electronically modified laboratory balance, which could not be adapted for chamber operation. Consequently, a high pressure combustion chamber had to be built and several major items of equipment procured and/or developed. The major items of equipment provided for the high pressure facility are described briefly below.

1. High Pressure Chamber:

The usual procedure used to minimize safety risk in high pressure oxygen experiments is to limit the experiment volume. This procedure was not feasible in this case since the ultimate experiment size and configuration were unknown and considerable viewing area was considered necessary. After several iterations, the final chamber configuration and interior volume was established. The interior dimensions were 12 cm in diameter by 23.5 cm in height. These dimensions would allow the manual placement and adjustment of specimens and support equipment, and pressure changes during the experiment would be small. Four equally

spaced ports were placed perpendicular to the chamber axis and four equally spaced ports were placed at 45° to the axis. Each port allows a circular viewing area of approximately 11.3 square cm at the sample. The ASME Unfired Pressure Vessel Code was used to determine minimum shell and closure dimensions. Considerable material was then added for additional safety (in case of wall combusion) and also to simplify casting of the item. Casting was used to eliminate welding. A sectional view is shown in Fig. 1 with Fig. 2 showing the finished chamber in position.

There were two critical chamber components. The first was the fire wall. This component must be capable of stopping a burning metal drop without being penetrated or cracking and exposing the chamber surfaces. Several configurations and materials were considered and tested. The configuration chosen was composed of several layers of heavy asbestos cloth heavily impregnated with a silicate refractory cement. The layers are applied wet and allowed to dry in place, providing a tight seal to the metal contours. The wall has been impacted a considerable number of times with molten burning material and impinged by the reflected laser beam without failure.

The second critical chamber component was the window for the laser beam. There are few materials which will pass 10.6 μm wavelength radiation. Of those that do, most have a large index of refraction and therefore require some type of antireflection coating. These coatings have two potential problems. The first was the possible adverse effect on the coating due to pressure stress. The second is radiation adsorption at particle adhesion points on the bottom surface. The energy adsorbed at these adhesion points could be sufficient to cause thermal cracking of the window and result in sudden window failure during an experiment. Because of the potential trouble with the higher strength high index of refraction materials, it was decided to use a low index of refraction uncoated

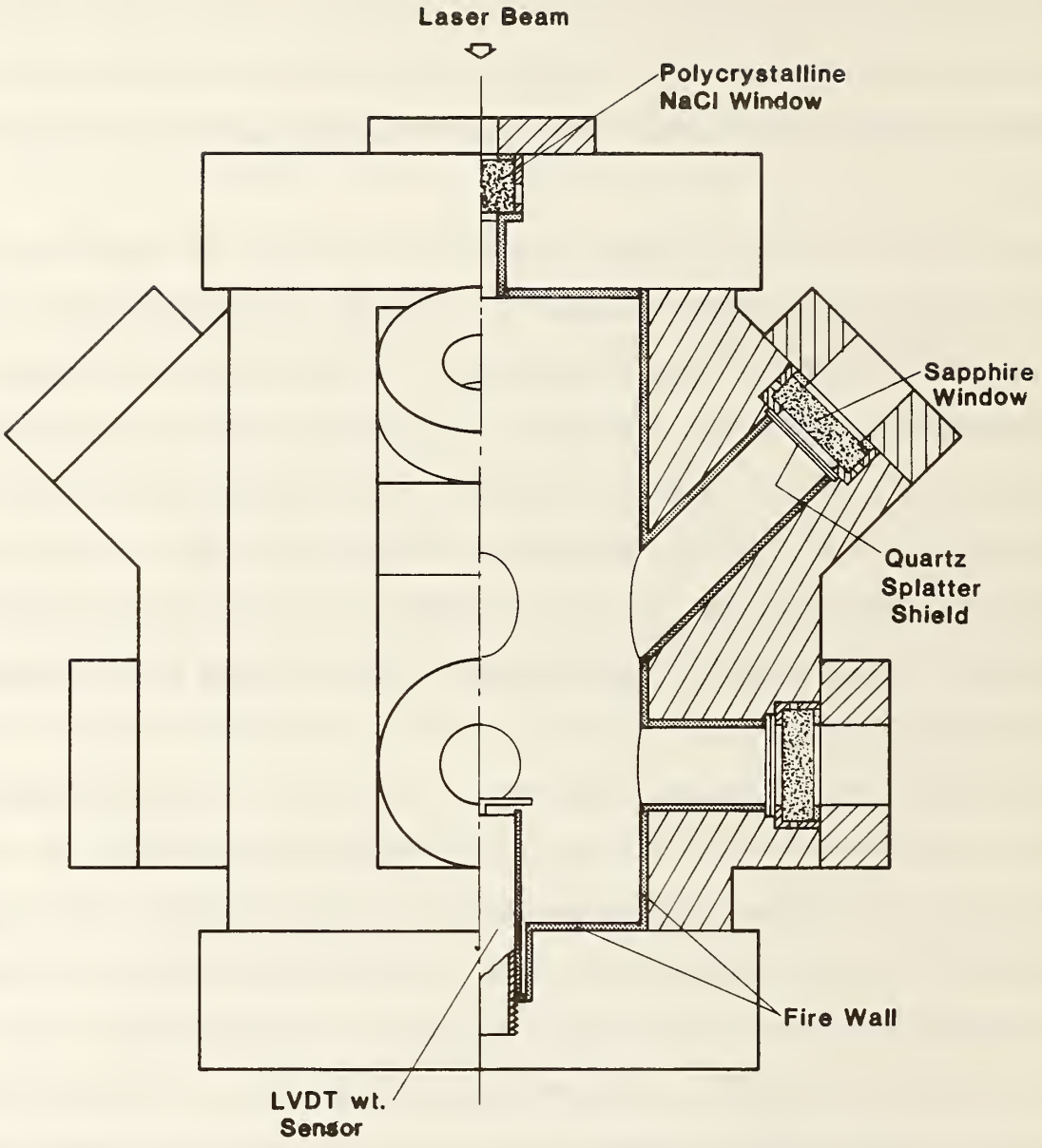


Figure 1. High pressure combustion chamber

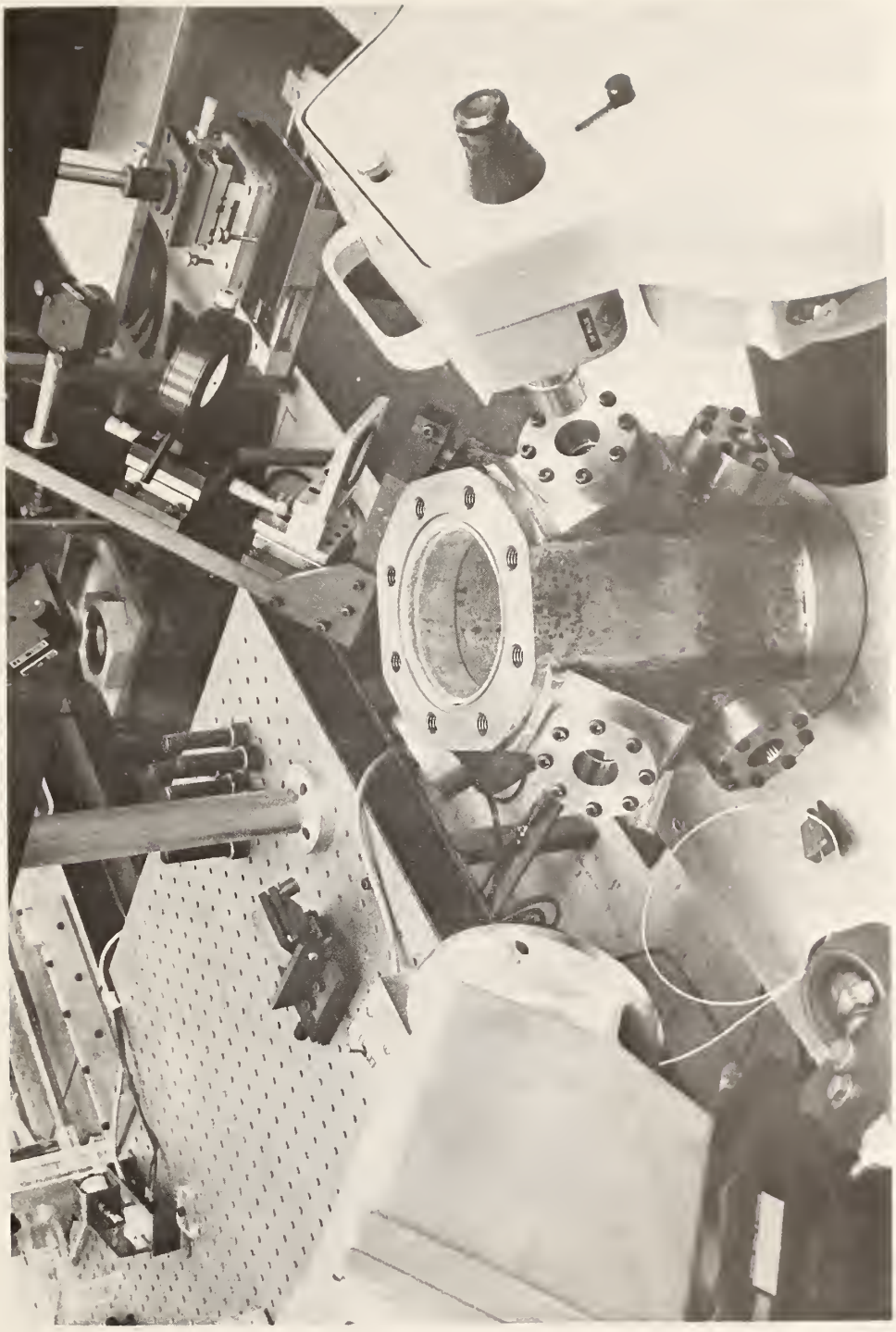


Figure 2. View of combustion chamber in position.

material, as a first attempt, even though this meant using a low strength material. The material chosen was polycrystalline sodium chloride. This material was readily available, relatively low cost, and potentially refurbishable. A window, using this material, was designed and several purchased.[2] The window has been tested to pressures of 14 MPa with no sign of failure even though considerable interior surface damage has occurred. It is expected that this item can be used to pressures significntly beyond 14 MPa. Figure 3 shows an exploded view of the window and mounting arrangement.

2. Surface Temperature Measurement

The experiment is arranged to allow the sample to be heated from the top. This top surface then will be the first to undergo ignition and combustion. To obtain an accurate temperature of this surface a noncontact method must be used. This prevents biasing of the temperature profile or changing the ignition temperature as would happen if a contact method was used. Infrared two-color ratio pyrometry was chosen as the means to measure the surface temperature. This two-color method differs from the method first chosen and reported in the first interim report. The method is discussed further in Appendix A.

Two pyrometers are used since energy spikes in the laser beam and convection currents from the sample generates moving hot spots. One pyrometer, a modified commercial unit, called a broadband pyrometer in this report, views the entire sample top surface. The temperature generated by this unit was an integrated average temperature and is called an average temperature in this report. The second pyrometer views a small area which can vary from 0.5 mm to 3 mm in diameter and is called a narrowband pyrometer in this report. A brief description of each pyrometer follows.

[2]Bransford, James W., Review of Scientific Instruments, Vol. 55, No. 1, pp. 125-126, January 1984.

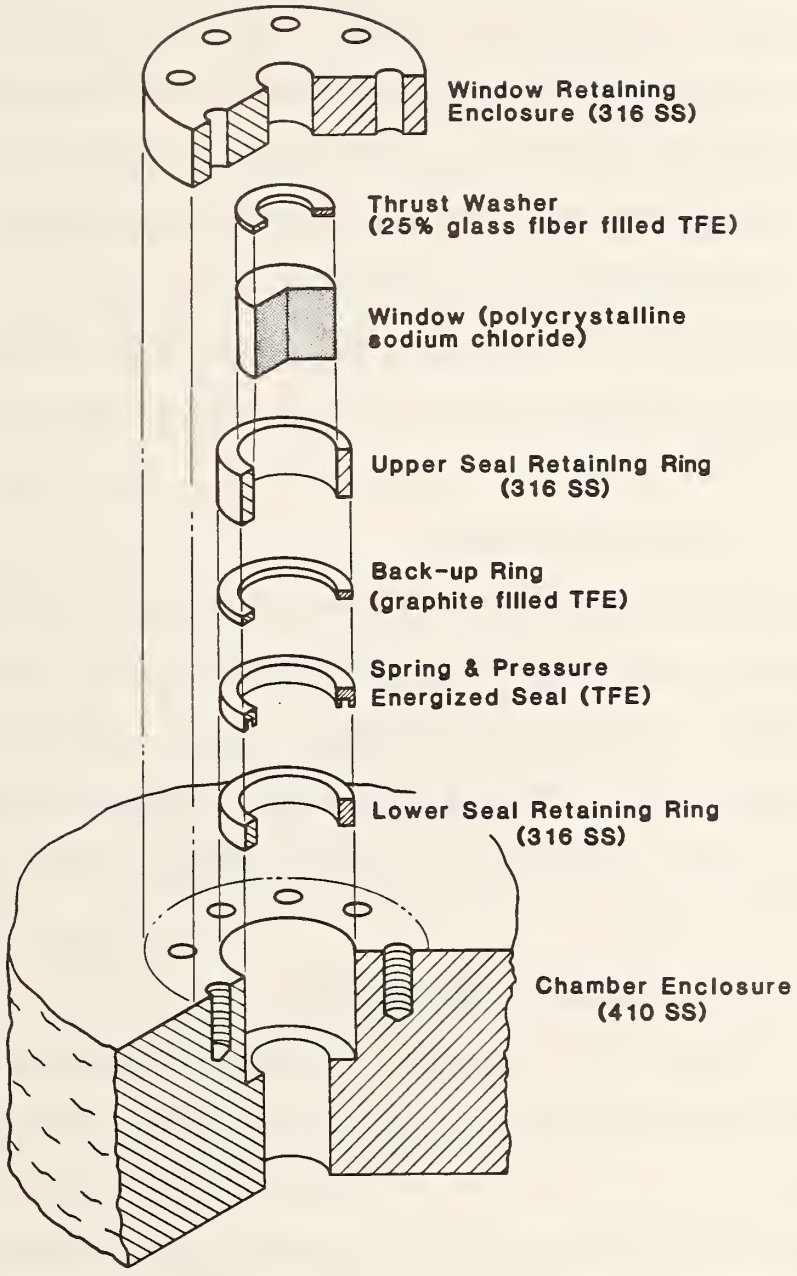


Figure 3. Polycrystalline sodium chloride window assembly.

a. Broadband Pyrometer

The broadband pyrometer was a commercial unit which has been modified to extend the valid temperature range from 1173 K to 2673 K. The field of view was approximately 6 mm in diameter at the sample, which covered the complete specimen top surface. The instrument was capable of making valid measurements with up to 95% signal attenuation (Appendix A). The spectral response range extends from 700 nm to 1050 nm with one signal derived from the entire spectral range centered at 950 nm and the second signal derived from a narrow wavelength band centered at 1050 nm. The accuracy of the instrument was typically 1% or better on smooth surfaces with some decreased accuracy on rough oxidized surfaces and surfaces that contain iron oxides.

b. Narrowband Pyrometer

The narrow band pyrometer was an in-house designed and constructed unit which operates on the same principle as the broadband unit. The major differences are that this unit has a narrow field of view and each signal's optical bandwidths are very narrow. The short wavelength signal was centered at 905.1 nm and the long wavelength signal was centered at 1060 nm. The bandpass for each wavelength was 10 nm FWHM.

3. Interior Temperature Measurement

It was considered highly desirable to have a specimen interior temperature in addition to the surface temperature due to the physical nature of the oxides produced during heat-up. The oxides of most of the alloys are tight protective oxides during much of the heat-up period. However, at the higher temperatures preceding ignition the oxide layer rapidly increases in thickness and develops a scaly or granular nature. This produces an insulating effect which may introduce a significant temperature differential between the upper oxide surface and the oxide-metal interface.

There are two techniques that can be used to measure an interior temperature in the ignition ranges expected. One technique, a blackbody radiant method, utilizes an iridium coated quartz fiber. The upper temperature limit is approximately 2000 K. The second technique utilizes a thermocouple. The measurement method chosen was the thermocouple since this device is less costly and easier to implement. Two types of thermocouples were used. They were tungsten 5% rhenium vs. tungsten 26% rhenium, which has the highest temperature capability but has oxidation problems, and platinum 10% rhodium vs. platinum which resists oxidation but has lower temperature capability. EMF data are available for temperatures up to 2593 K for the tungsten system and to 2041 K for the platinum system. Wire diameter for each thermocouple system was 0.13 mm (0.005 in).

4. Mass Measurement

The metals and alloys of this study produce nonvolatile oxides which remain mostly within the reaction zone. Thus, if a sufficiently sensitive mass measurement device can be found and a stable baseline maintained during the experiment, the rate of the oxidation reaction can be followed. Two mass sensors have been used, one exclusively for the open atmosphere experiments, and one exclusively for pressure chamber experiments.

The mass sensor used for the open atmosphere experiments was a standard laboratory electronic balance. The balance electronics were modified to increase the response time and to stabilize and amplify the output signal. The sensitivity of this unit was 10 mg/mV.

The second mass sensing unit, which was used for experiments in the pressure chamber, is based upon an LVDT force transducer. This device was modified to withstand pressures up to 70 MPa. The unit has a full scale range of 100 grams. In use, the output signal is offset and amplified to give a sensitivity of approximately 6 mg/mv. The unit has one drawback. The spring mounted platen

assembly is undamped and thus was very sensitive to vibration and impulse loads produced during combustion. Never-the-less, the precombustion oxidation rate can be obtained with good accuracy.

B. Experiment

1. Materials

For this effort, the materials consisted of eighteen metallic alloys and three nonmetallic materials. A list of these metallic alloys and their chemical composition is given in Table 1. Several other materials will also be included in this study. These will provide a link to previous experiments and also provide information on the behavior of several pure materials which form the basis for the alloys being studied as well as several other alloys of interest. Several of the additional materials that will be studied are pure iron, pure nickel, monel 400, monel K-500, and pure copper. As the results of previous work are compiled, other materials may be added.

2. Specimen Geometry

The original study utilized small irregular-shaped specimems cut from sheet stock. This type of specimen does not lend itself well to accurate interior or exterior temperature measurements; thus a change in specimen geometry was necessary if these data were to be obtained. It was also desirable to change the specimen geometry in order to increase the mass data signal-to-noise ratio.

In arriving at an applicable specimen geometry, several requirements had to be kept in mind. These were:

1. Maximum laser power was between 75 to 85 watts.
2. Ultimate specimen temperature needed to approach 1800 K or higher for the iron, nickel, and cobalt alloys and to exceed 2330 K for the aluminum alloys in order to be assured of reaching an ignition temperature.

	Al	B	C	Cb Ta	Co	Cr	Cu	Fe	Mg	Mo	Mn	Ni	P	S	Si	Ti	V	W	Zn	Zr	Other
A-358[1]	Bal						0.20	0.20	0.25-0.45		0.10				6.5-7.5	0.20			0.10		0.15
Tensile-50	Bal					<0.2	<0.2	<0.4	0.4-0.6						7.6-8.6	0.1-0.2			<0.2		0.1-0.4
301 SS[1]			0.15			16-18		Bal			2.0	6-8	0.045	0.030	1.0						
302[1]			0.15			17-19		Bal			2.0	8-10	0.045	0.030	1.0						
304[1]			0.08			18-20		Bal			2.0	8-10.5	0.045	0.030	1.0						
304L[1]			0.03			18-20		Bal			2.0	8-12	0.045	0.030	1.0						
318[1]			0.08			16-18		Bal		2.0-3.0	2.0	10-14	0.045	0.030	1.0						
321[1]			0.08			17-19		Bal			2.0	9-12	0.045	0.030	1.0	5•C[3]					
347[1]			0.08	10•C[3]		17-19		Bal			2.0	9-13	0.045	0.030	1.0						
A-286[2]	0.22	0.008	0.027			13.88	0.03	Bal		1.25	1.13	24.47	0.021	0.001	0.42	2.17	0.220				
440 C[1]			0.95-1.20			16-18		Bal		0.75	1.0		0.040	0.030	1.0						
Nariloy A												Bal									Ag 3.5
Haynes 188[1]			0.10		Bal	22		3			1.25	22			0.3			14			La 0.04
Hastelloy[2] C 276			0.003		1.87	15.90		6.20		15.30	0.50	Bal	0.009	0.003	0.03		0.10	3.27			
Waspaloy[2]	1.27	0.005	0.03		12.49	19.21	0.02	0.75		4.22	0.01	58.82	0.002	0.003	0.02	3.13				0.048	
Inconel 825[2]	0.17		0.04	3.90		22.10		2.44		8.77	0.03	62.38	0.005	0.002	0.02	0.28					
Inconel 718[2]	0.49	0.002	0.04	5.22	0.08	18.08	0.20	18.17	<0.01	2.99	0.18	53.44	0.007	0.002	0.02	0.83					Ca <0.01
Inconel[2] X 750	0.82		0.028	0.79	0.02	15.38	0.01	7.93			0.11	72.08	0.007	0.001	0.07	2.80					

1. Normal composition, single number is maximum allowed.
2. Ladel analysis
3. Minimum amount

Table 1. Material composition.

3. Heat-up time to maximum temperature needed to be kept to less than three minutes maximum, and preferably to about two minutes.

Several specimen configurations and dimensions were tried. A cylindrical specimen with height equal to diameter (5 mm), to minimize heat loss by radiation, was found to meet most of the above requirements adequately and give consistent results. A 0.635 mm diameter thermocouple well was drilled axially to within 0.25 mm to 0.40 mm of the top surface. The thin web of material at the top of the specimen requires that the experiment be completed beyond the point of ignition before normal nonprotective oxidation completely destroys the web and also the thermocouple. This destruction of the web by the nonprotective oxidation mechanism usually requires two to three minutes after reaching high temperature. The thermocouple will sense an environment which is hottest directly above the bead but cooler at the sides. The temperature measured by the thermocouple was an "averaged" temperature biased slightly to the low side from the true oxide-metal interface temperature.

3. Experimental Arrangement

The experimental set-up for the open atmosphere experiments and the pressure chamber experiments was essentially the same. The major difference was that the spray shield for the open atmosphere set-up had a smaller top opening for the laser beam and oxygen was introduced through a small side opening with flow across the top of the sample. Figure 4 shows a side view of the pressure chamber set-up. The mass sensors were utilized as the experiment support and were protected from excessive heat by a foam fire brick. A graphite crucible was used to contain the specimen and molten material produced during combustion. Heat transfer from the specimen to the crucible must be minimized in order to achieve the desired heating rate and maximum temperature. To achieve this, the thermocouple was bonded in place in the specimen well in the graphite block. Then the

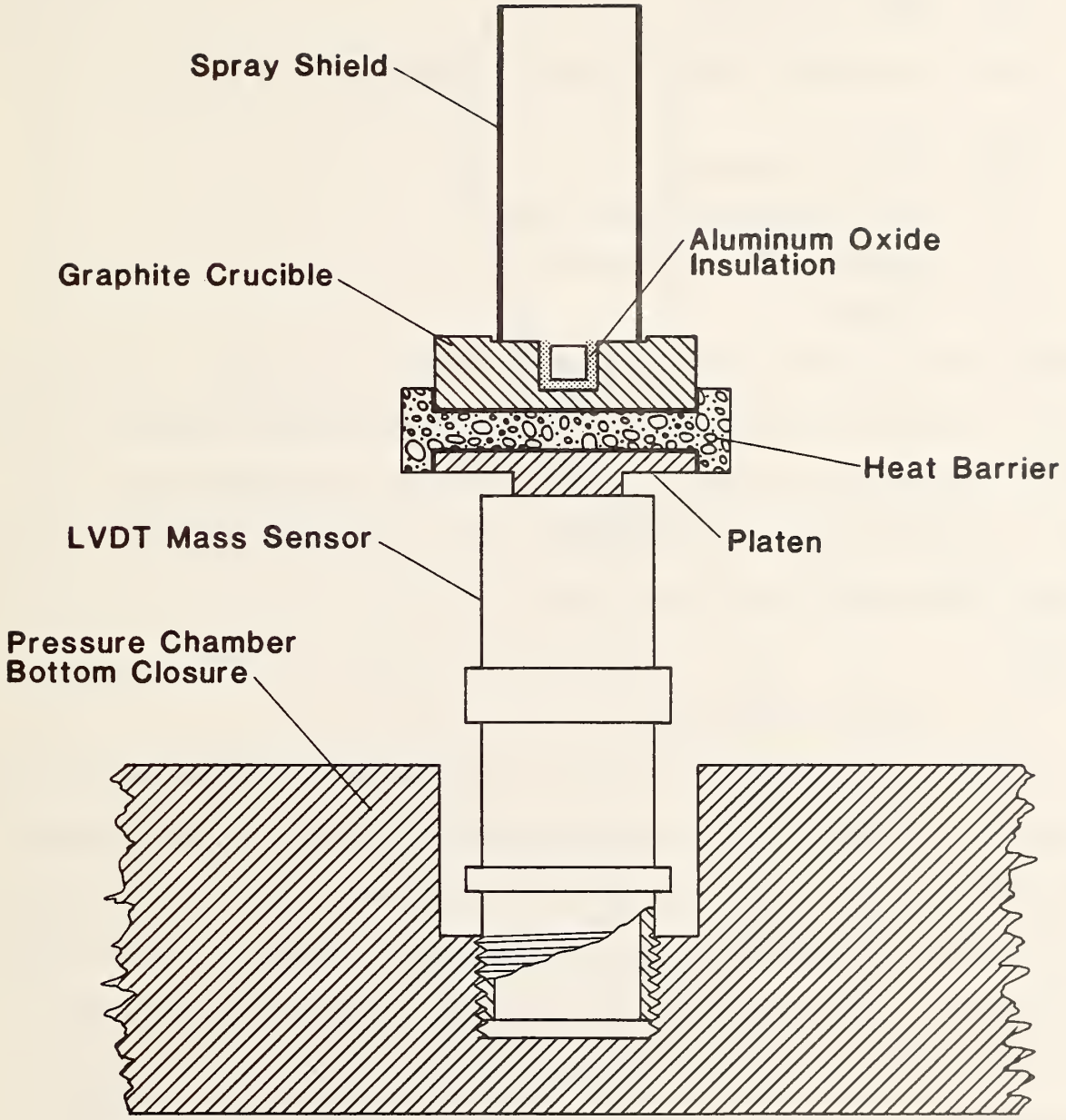


Figure 4. Experimental set-up in combustion chamber.

specimen well was lined with packed aluminum oxide powder to a thickness of approximately 1 mm on the side and 2 mm on the bottom. The specimen was then inserted firmly over the thermocouple and seated firmly on the aluminum oxide powder. The thermocouple leads are then connected to the chamber feed-thru leads and the mass sensor calibrated.

A typical experiment records at least five quantities which are:

1. Mass
2. Interior temperature
3. Overall top surface temperature
4. Spot top surface temperature
5. Brightness

High-speed movies and/or spectral measurements may also be made. All electronic data were recorded on digital oscilloscopes with the possible exception of spectral data which can be recorded as digital, analog, or photographic data. All digital data were passed through a desktop computer for processing and recording onto permanent magnetic tape or disc files.

III. RESULTS

A. Specimen Heating Rate

A number of specimens of several alloys representative of the overall group of materials were heated in air to confirm that the desired maximum temperature range could be reached in the required time. (Air contains sufficient oxygen to give an oxidized surface similar to that obtained in pure oxygen without supporting combustion). The thermocouple was positioned at the predetermined depth of 0.25 mm to 0.40 mm from the top surface as well as at other positions. The surface temperature was measured using the broadband pyrometer. The results of these heating experiments were compared to computer generated temperature distributions and heating rates. Two comparisons were made, one for the high thermal

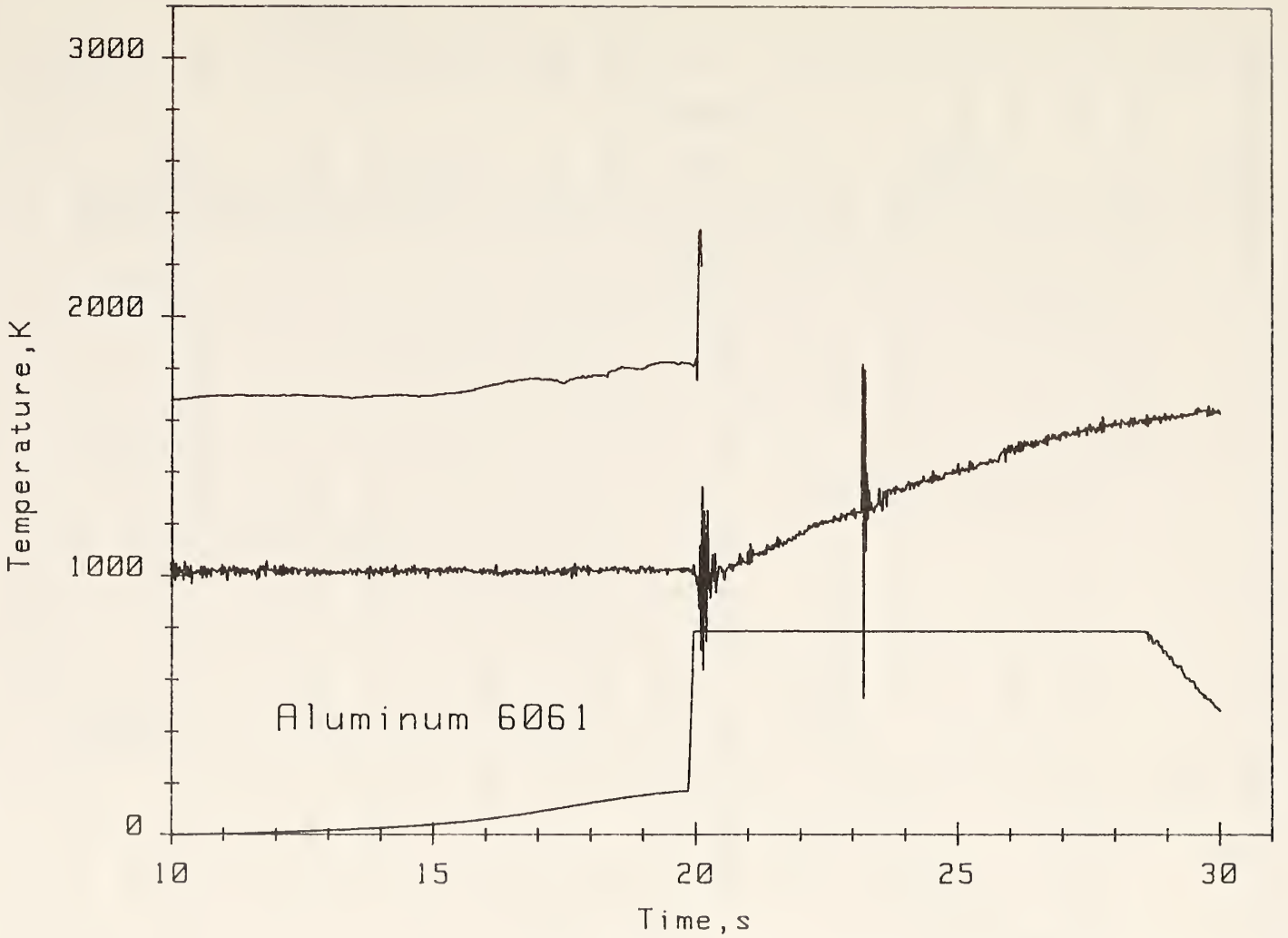


Figure 9. Typical signals for an aluminum 6061 combustion in atmospheric flowing oxygen.

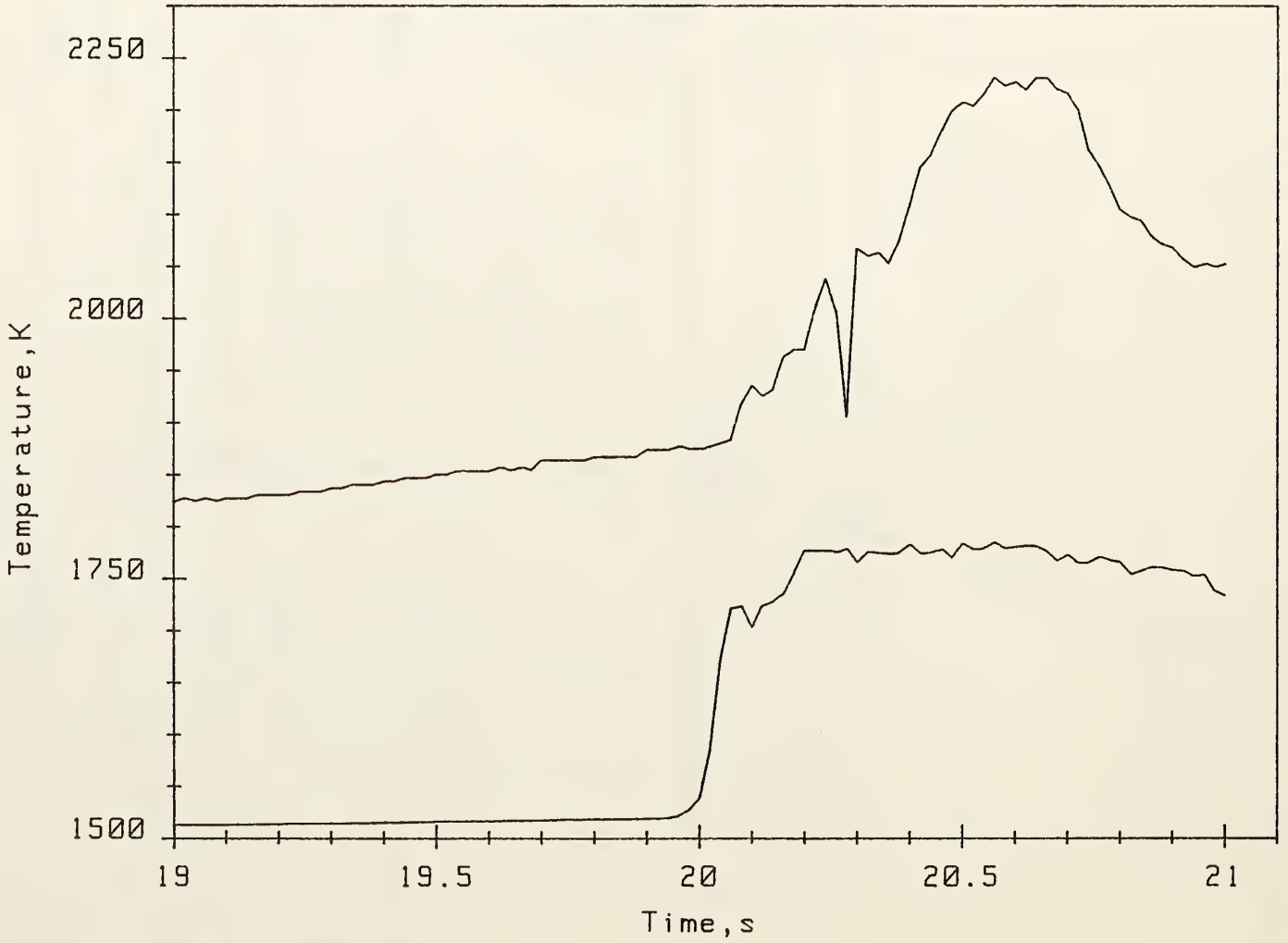


Figure 10. Expanded results at ignition for aluminum 6061.

ignition, and the ignition temperature determined from this trend curve. However, this procedure was used only if the data are considered to be extrapolatable. The values obtained for the temperatures at ignition for aluminum 6061 ranged from approximately 1700 K to approximately 2100 K with most data above 1825 K.

2. Iron and Nickel Base Alloys

The ignition and combustion behavior of the larger specimens, 750 mg and heavier, used in this phase of the program, was essentially the same as for the smaller specimens used in the initial study. A small hot spot would develop within the laser beam impingement area and then develop into combustion and spread across the specimen surface. All of the iron and nickel alloys studied could be ignited and would burn to completion. Monel 400 and Monel K-500 could also be ignited and would burn to completion. Nickel 200, essentially pure nickel, was the only material that could not be reliably ignited. This was due to the development of a heavy layer of nickel oxide which has a very high melting point, 2363 K, and thus prevented oxygen transport to the molten metal. In fact, if the experiment run time was lengthened at the higher temperatures, the heavy build-up of oxides could prevent ignition of all of the materials studied.

The determination of the ignition temperature, for this phase of the study, was a major problem since a surface temperature measurement was not available. Previous investigators had used the most rapid rate of change in the brightness signal ($ds/dt = max.$) as the time reference in determining the ignition temperature. To test this definition against oxidation rate data, a number of experiments were run in which the brightness signal was correlated with the mass signal. Figure 11 is a typical result for a stainless steel. It was found that generally ds/dt was a maximum during combustion, not at ignition, and therefore could not be used to determine the time at which ignition occurred. To further

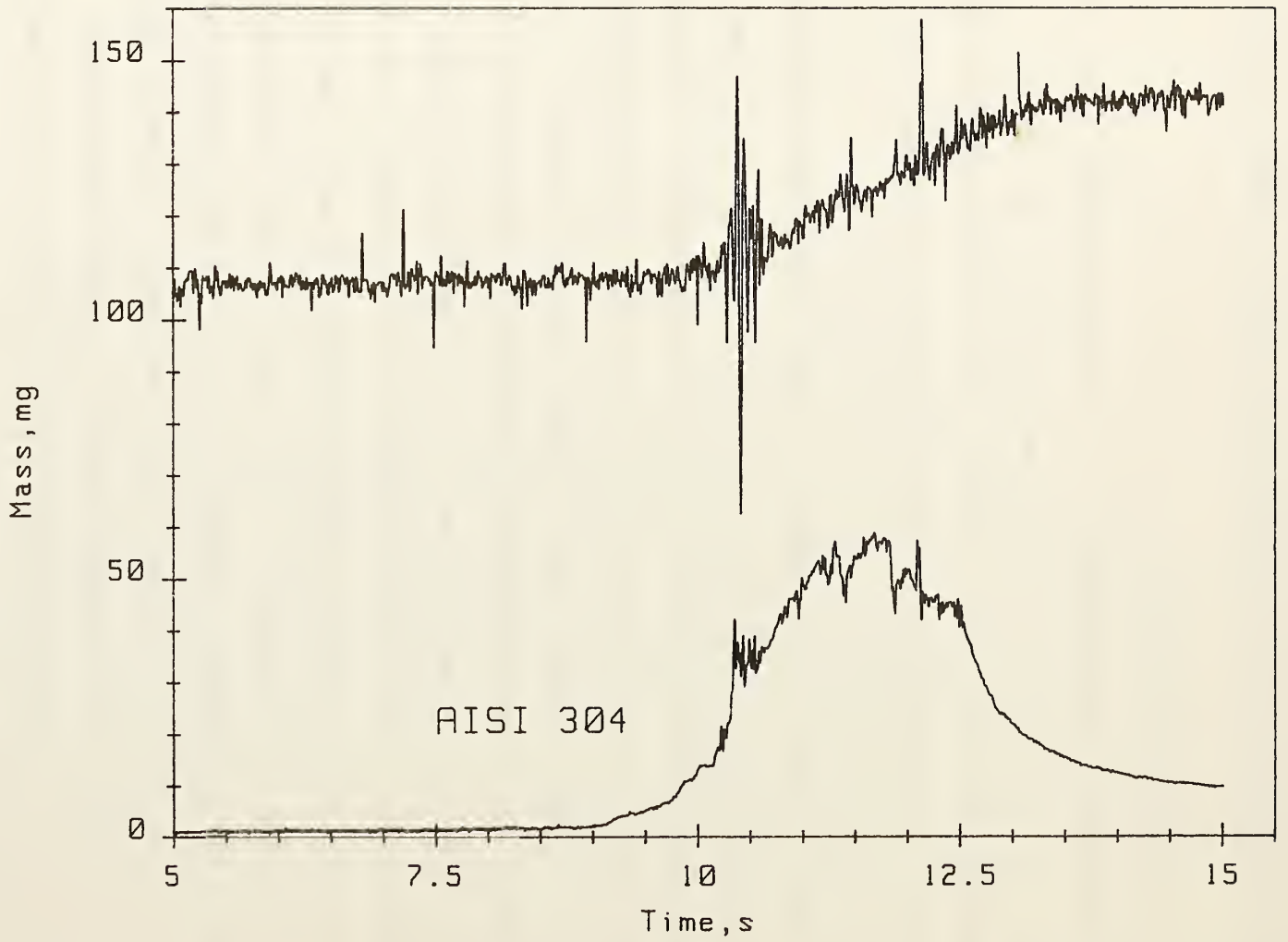


Figure 11. Brightness and mass correlation for an AISI 300 series stainless steel.

complicate the problem, there was an experiment-to-experiment and a material-to-material variation in the specific detailed shape of the brightness curve as well as the relation of the curves general features to the oxidation rate curve.

The problem presented by the inconsistent brightness curve is partly resolved by using mass data to determine the beginning of combustion and then working backward to determine the most probable time for ignition to have occurred. This procedure requires that the ignition reaction continue sufficiently long to consume a detectable amount of material. For most of the materials studied this criterion appeared to be met; however for several, the product oxides suppressed adequate consumption of material so that ignition point could not be estimated from the mass curve.

Figure 12 shows the relationship between interior temperature (upper curve), weight (middle curve), and brightness (lower curve) obtained from the combustion of a 650 mg specimen of 304L stainless steel. This data set was representative of those obtained from all 300 series stainless steels. For this test, the oxidation rate began to accelerate at five seconds. Since there was an absence of any indication of abrupt surface temperature transitions prior to this time, ignition was assumed to occur at that time.

The results of the atmospheric flowing oxygen experiments can be grouped according to alloy type, i.e., 300 series stainless steels, nickel based alloys, etc. These results are summarized below.

a. Stainless Steel: AISI 302, 304, 304L, 316, 321, and 347

Based upon oxidation rate data, these alloys appeared to ignite within their respective melting ranges, 1672-1728 K, with some data indicating ignition temperatures may be as low as 1600 K. Unsupported combustion was not concurrent with ignition; the alloys must be in the liquid phase in order for unsupported combustion to occur.

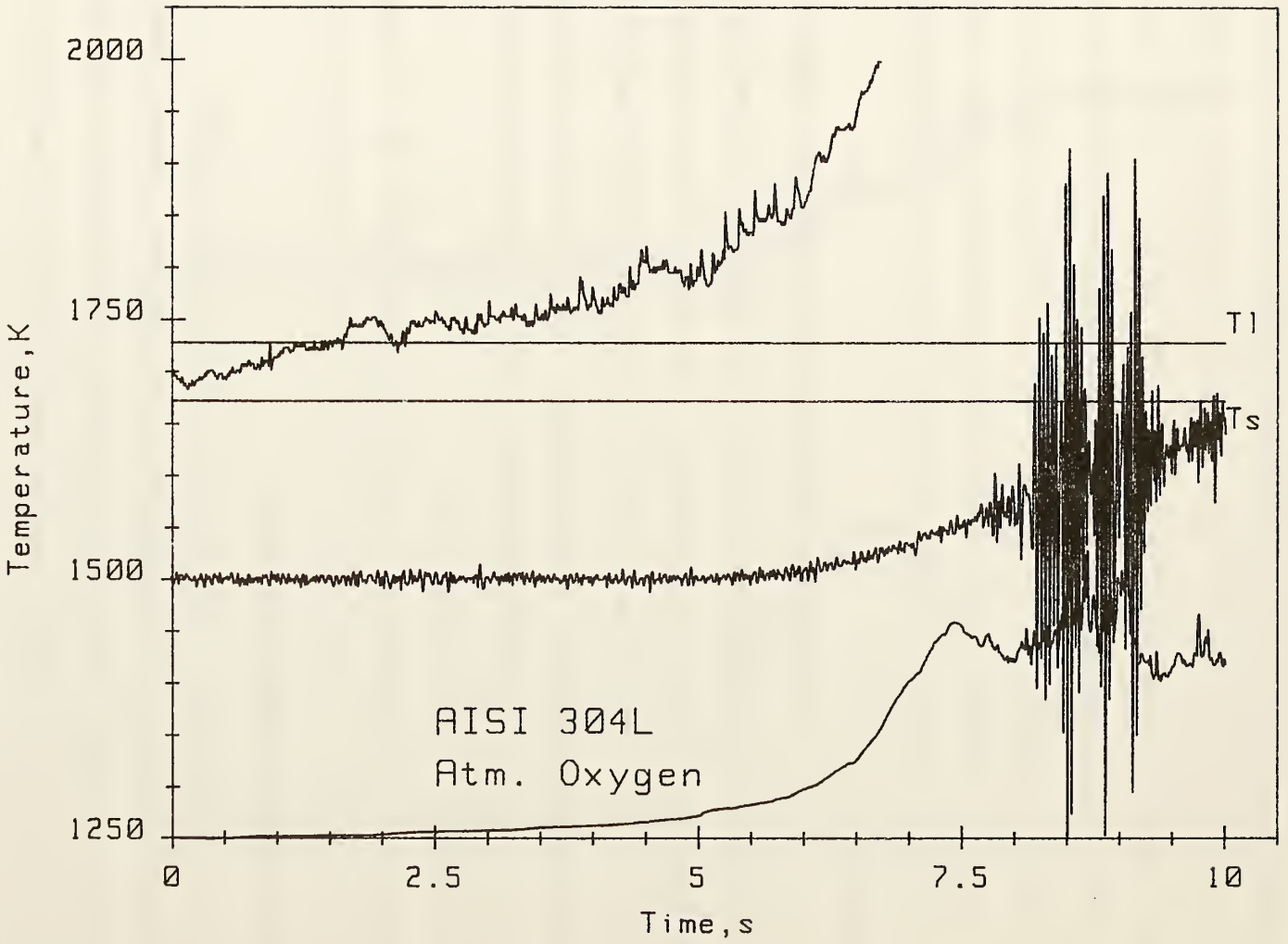


Figure 12. Typical results for an AISI 300 series stainless steel in flowing oxygen.

b. 440C Stainless Steel

This was the only 400 series stainless steel tested. The data indicate a probable broad ignition range with a low end approaching that of pure iron, approximately 1400 K, but with definite ignitability in the liquid phase, 1644-1783 K. Unsupported combustion can only occur if the alloy is liquid, greater than 1600 K.

c. Nickel Based Alloys: UNS N06600, N06625, and N07718

These alloys typically ignited within their respective melting ranges, 1533-1700 K. Some data indicated ignition at slightly less than the solidus temperature. Unsuported combustion can only occur if the alloy is fully liquid.

d. Monel 400 and K-500

The data for these two alloys are erratic, but ignition appears to occur at temperatures greater than 1500 K, with combustion occurring in the liquid phase.

C. Ignition and Combustion Test in Pressurized Oxygen

The ignition and combustion characteristics for the vapor burning alloys did not change with increasing oxygen pressure. However, for the liquid surface burning alloys, there were two significant changes in behavior. The most noticeable change occurred in the amount and size of the droplets and spray which is ejected during combustion. The increased pressure decreased the size of vapor bubbles which drive the droplet and spray mechanism. This allowed the vapor bubbles to accumulate and build in size until a critical size was reached. This critical size then overcomes the surface tension, which maintains a stable fluid volume, expands and literally blows the molten sample from the crucible in large drops. The most severe action occurred in the 0.34 MPa (50 psia) to 0.69 MPa (100 psia) pressure range. For pressures greater than 1.38 MPa (200 psia) the ejection of large droplets of material was essentially suppressed for the specimen size used.

The second change in behavior occurred in the ignition sequence. In general, the surface temperature at ignition experienced a sharp increase (Figure B.3) and the time between the development of an ignition zone (hot-spot) and the development of full combustion was considerably shorter than in the atmospheric tests. For some cases, the delay between ignition and combustion was only a few data acquisition time periods and could be considered to be concurrent.

The results of the testing, to date, at elevated pressures is presented in the following sections.

1. Aluminum 6061

Aluminum 6061 is the only aluminum based alloy tested at elevated pressure to date. It was possible to obtain data on this alloy to pressures of 2.41 MPa (350 psia) but not beyond, due to sample cooling by the higher density gas. An interesting and unexpected event occurred during this series of tests. Longer than normal heating times had to be used to reach ignition temperature; several of these tests failed to ignite and the tests were terminated; however, during cool-down the specimen ignited and burned. These data points are marked by circles in Figures 13 and 14. It is thought that a stress fracture developed in the oxide shell exposing the molten metal. The energy of the resulting surface oxidation reaction was trapped within the crack and raised the temperature of the immediate material to the ignition point, causing ignition and combustion. Figure 15 presents the data from both pyrometers for one such event. The top curve shows the narrowband pyrometer data; the bottom curve, the broadband pyrometer data.

Figure 13 presents the average top surface temperature at ignition. As can be seen there is a slight ignition temperature decrease, 9.12 K/MPa (0.0629 K/psi), at pressures beyond 0.14 MPa (20 psia). Figure 14 represents

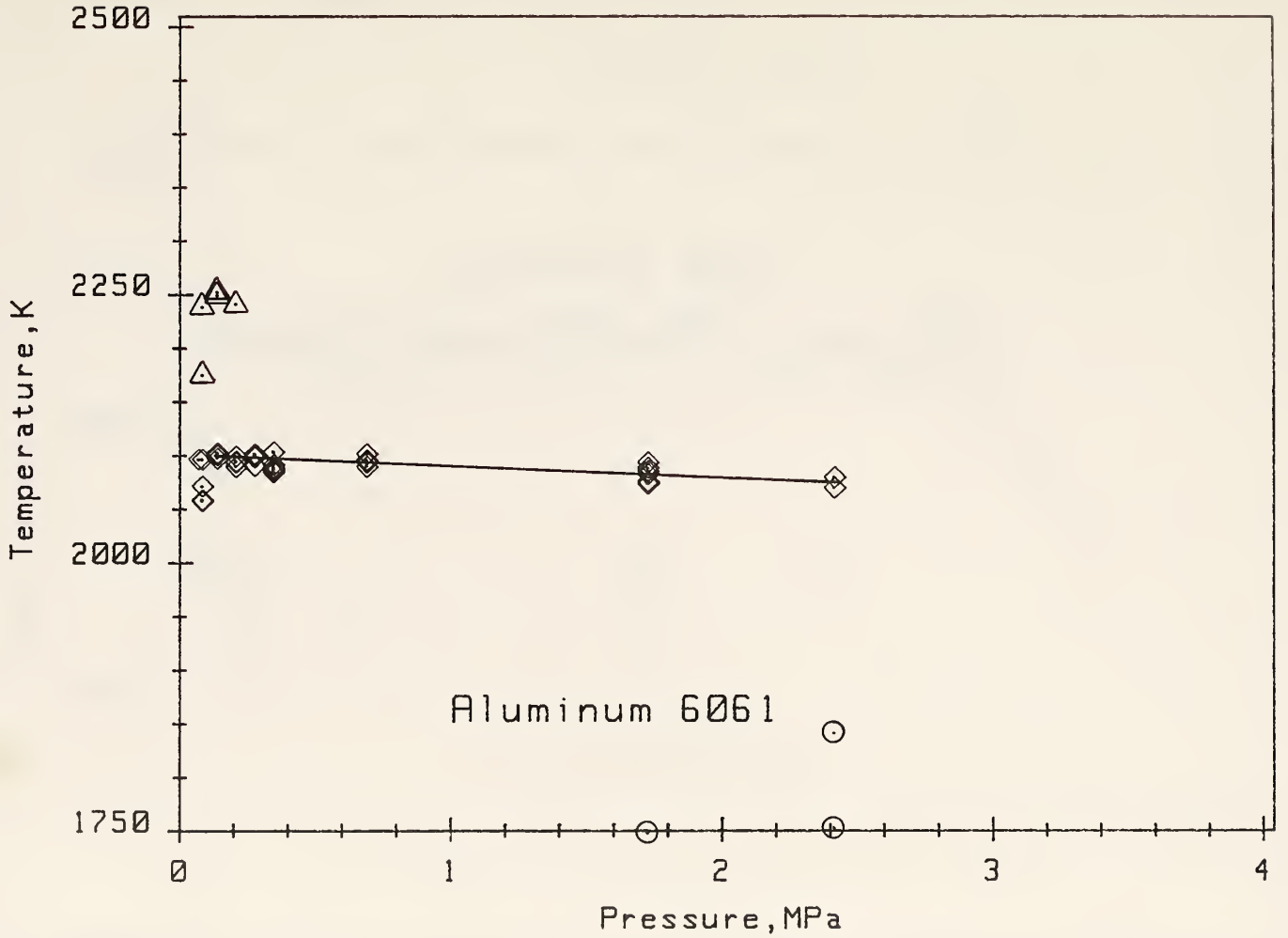


Figure 13. Average surface temperature at ignition for aluminum 6061.

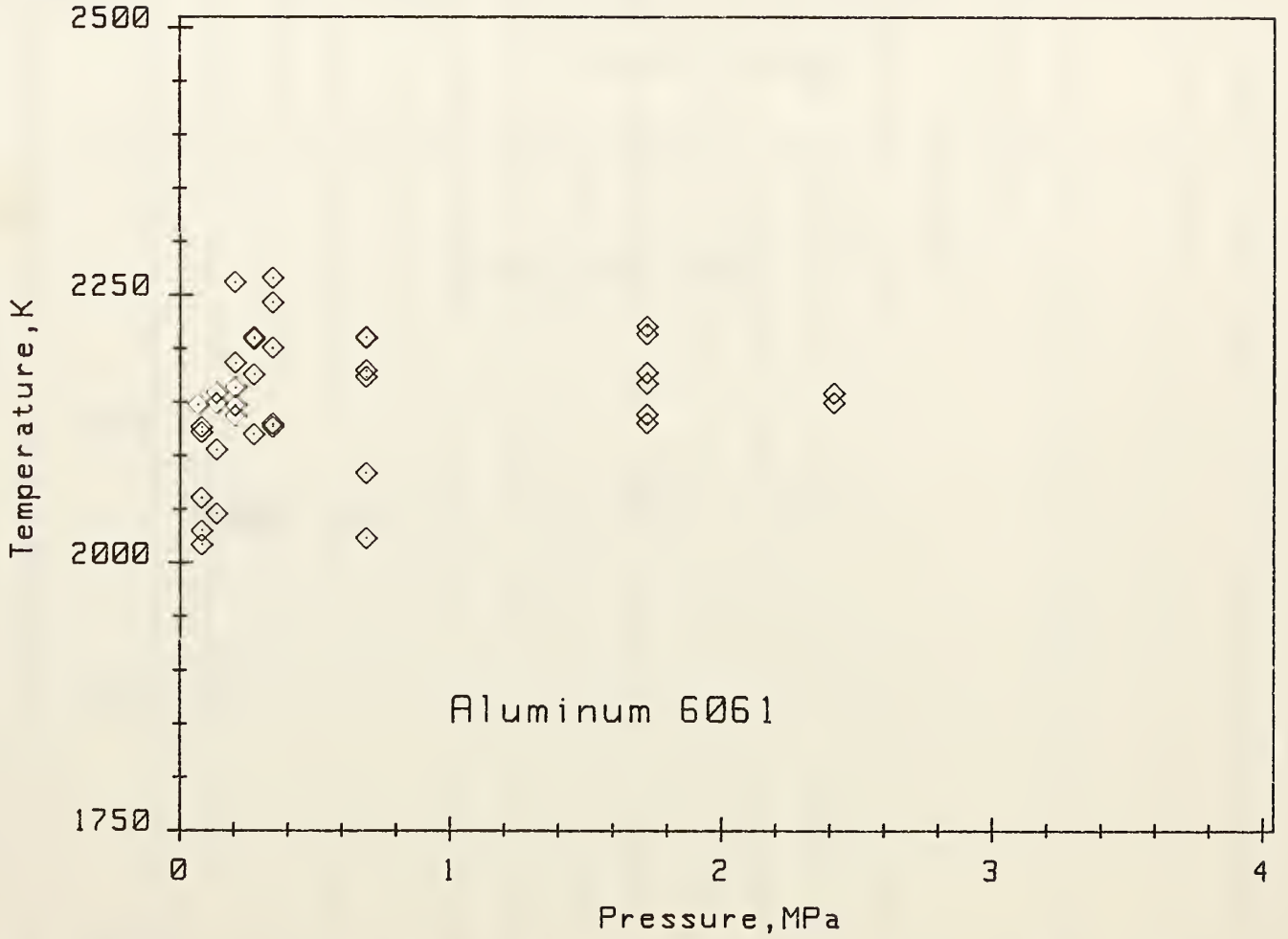


Figure 14. Temperature at ignition for a 0.5 mm diameter surface area for aluminum 6061.

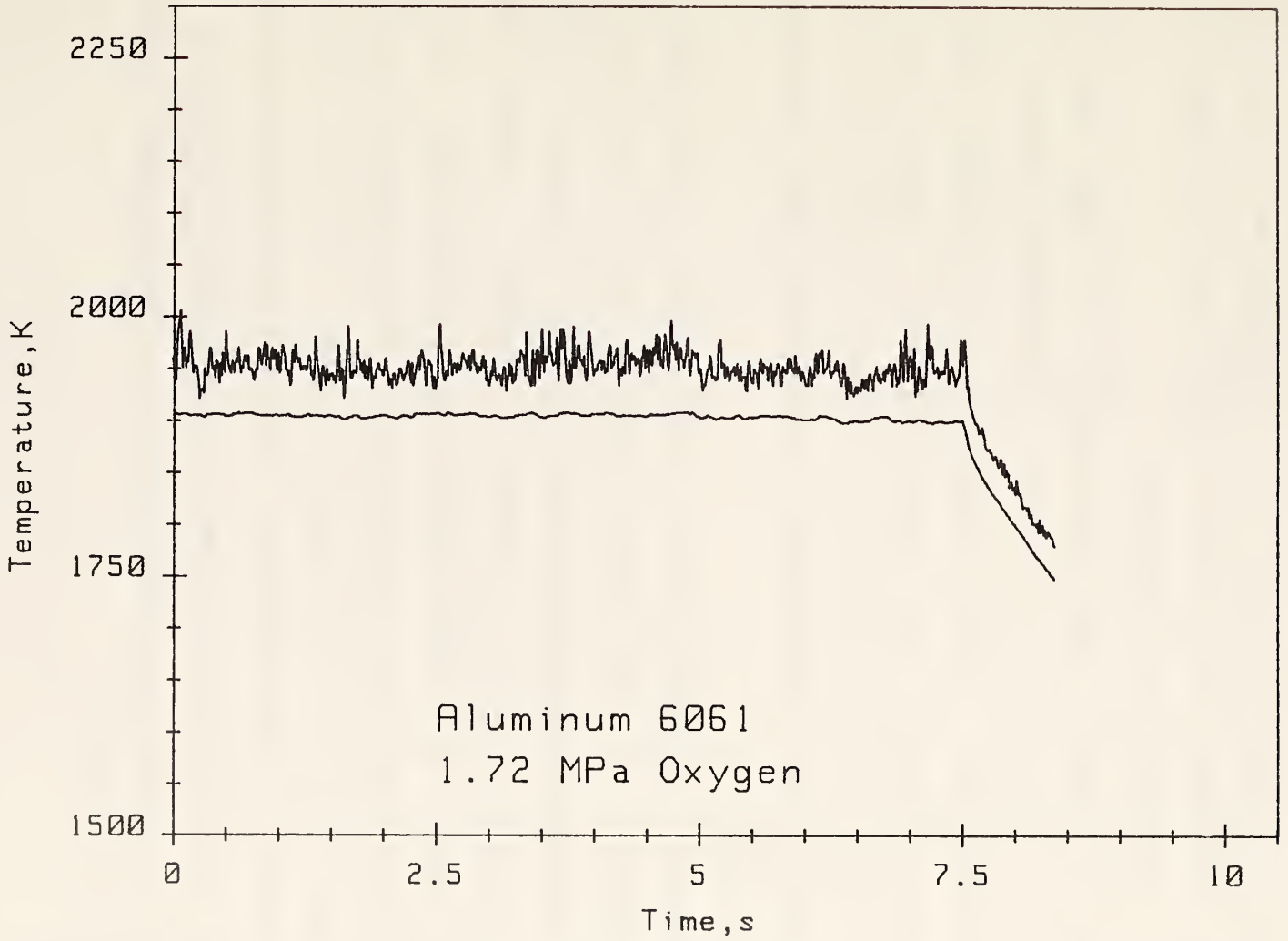


Figure 15. Surface temperatures of aluminum 6061 for an ignition on cool-down.

the temperatures of a 0.5 mm diameter area on the top surface at ignition. This data shows the variation that can exist in surface temperatures. Maximum surface temperatures are considered to be approximately 150-175 K above the average surface temperature linear least squares curve. The temperature of the oxide-alloy interface is considered to be within $\pm$20 K to the linear least squares curve.

2. Cobalt-Based Alloy, Haynes 188

Haynes 188 was the only cobalt-based material to be tested. Material in suitable configuration could not be obtained. Specimens were therefore cut from flat stock and stacked. This type of specimen only allowed surface temperatures to be measured. From the existing data and examination of samples that did not ignite, it appears that the material must be within the melting range, 1575 to 1630 K or above to ignite, and definitely must be fluid in order for unsupported combustion to occur.

The material is extremely difficult to ignite due to the thick oxide layer produced during heat-up. This oxide layer appears to have a melting range significantly above that of the alloy and thus restricts heat transfer to the base alloy, preventing easy ignition and combustion. A number of attempts to ignite the samples failed. These samples sustained severe surface damage, i.e., oxidation, melting and vaporization, without burning. Ignition temperatures (see Appendix B) were difficult to obtain because the nature of the oxide layer required extended run times to obtain combustion. Those that were obtained are presented in Figure 16 while temperatures at combustion are presented in Figure 17. These temperatures are probably considerably higher than the oxide metal interface because of the oxide thickness.

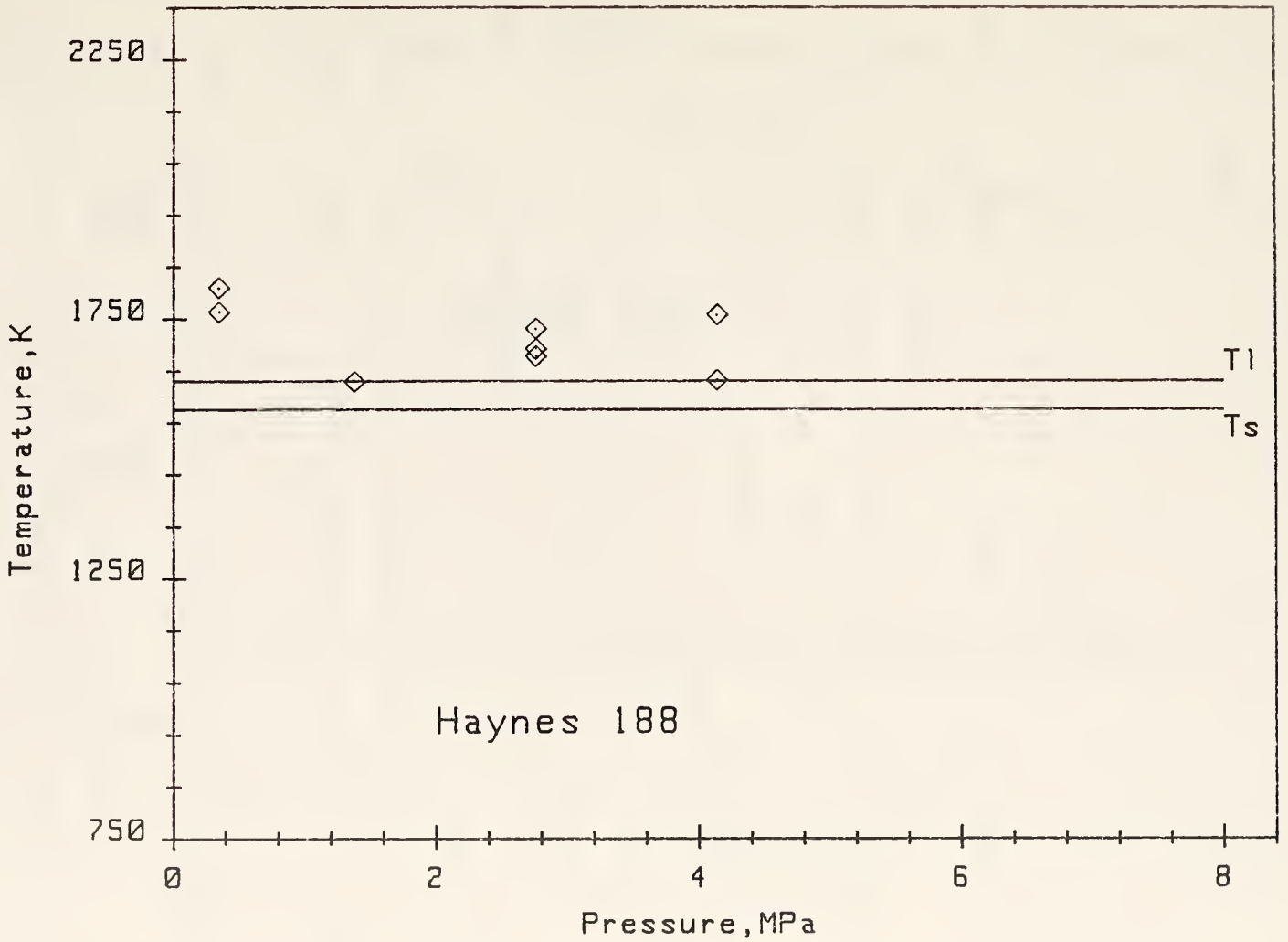


Figure 16. Average surface temperature at ignition for Haynes 188.

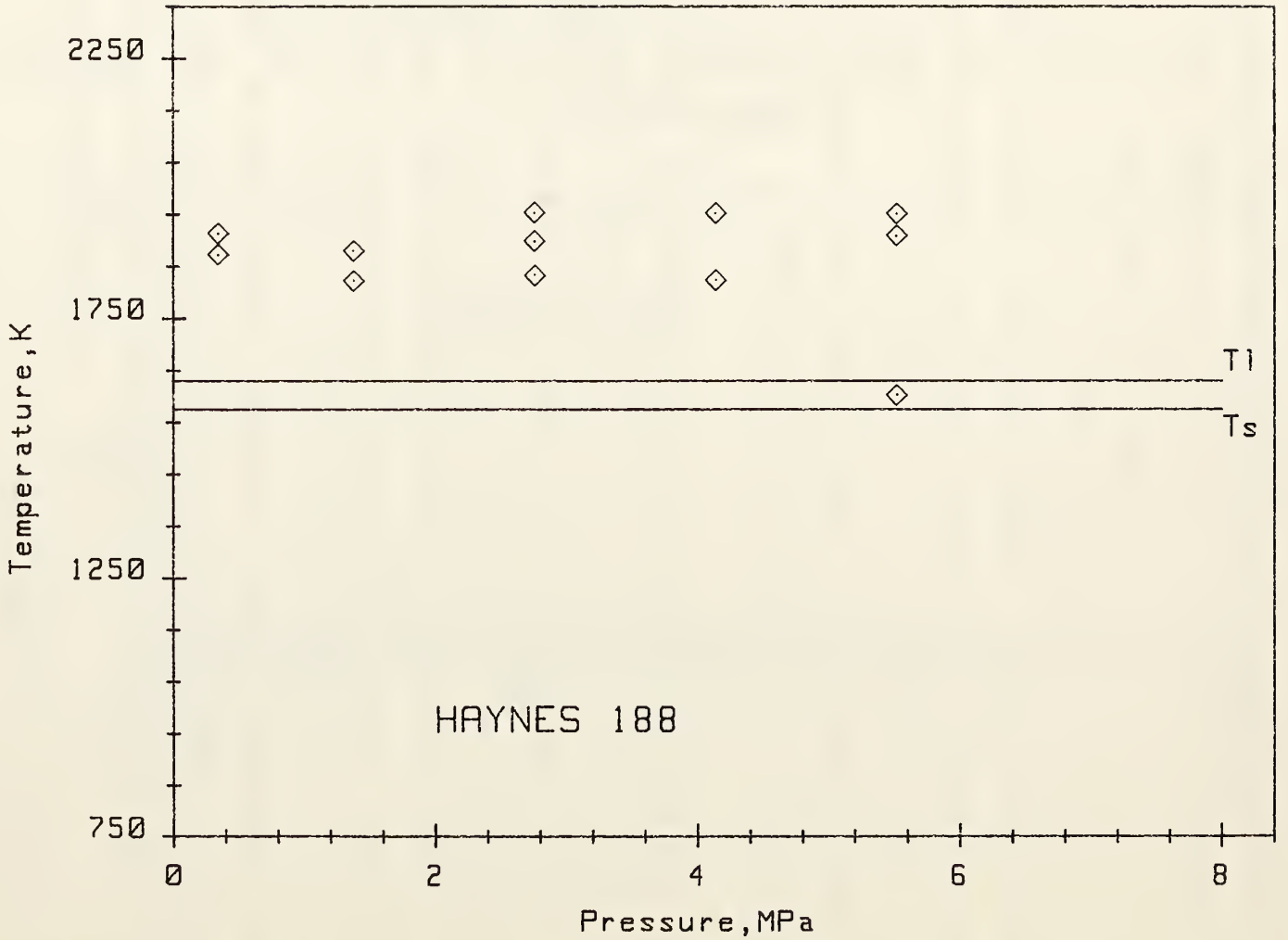


Figure 17. Average surface temperature at combustion for Haynes 188.

3. Iron-Based Alloys

a. Carbon Steel 1018

A carbon steel was included since atmospheric flowing oxygen tests had indicated that the 300 series stainless steels may ignite below the solidus temperature. It was thought that ferrous oxide, carbon or iron-carbides were the most probable source of the ignition. Since many of the materials to be studied contain significant quantities of iron, and some carbon, it was considered expedient to determine the ignition and combustion characteristics of an iron-carbon system for comparison to other iron containing alloys. Carbon steel 1018, which was readily available in the laboratory, was used for this work.

The temperature data from the broadband pyrometer shows considerable regional surface temperature activity. Temperature spikes are apparent from the activation of this instrument at approximately 1173 K until combustion begins. Mass data, however, indicate that little or no detectable mass was consumed prior to ignition. Consequently, these temperature spikes are not considered to be ignition zones but may be due to the rapid heating of loose oxide layer scales or the ignition of microscopic phases on the specimen surface. Combustion develops rapidly from a major ignition event. Figure 18 presents the interior temperature data and Figure 19 the average surface temperature data at ignition. There is a slight pressure dependence in ignition temperature with increasing oxygen pressure, but not large enough to be considered significant at this time. Rapid combustion occurs only in the fluid state. Ignition and combustion may be considered to be concurrent.

b. Stainless Steel: AISI 302, 304, 304L, 316, 321, and 347

The detectability of the ignition point of the AISI 300 series alloys tested improved dramatically with increased oxygen pressure, Figure B.3. The ignition temperatures also decreased to within the melting range or below, if the solidus

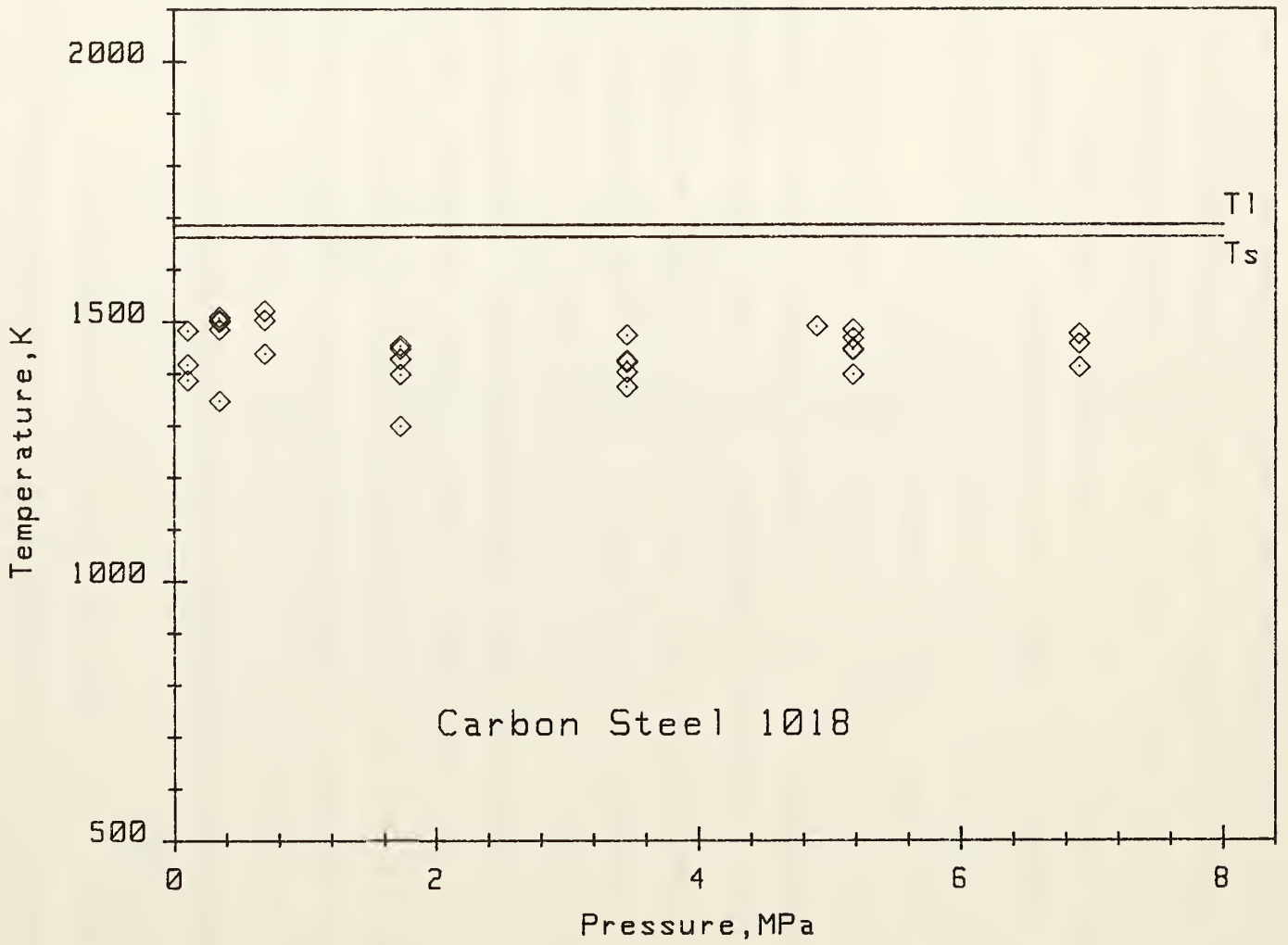


Figure 18. Interior temperature at ignition for carbon steel 1018.

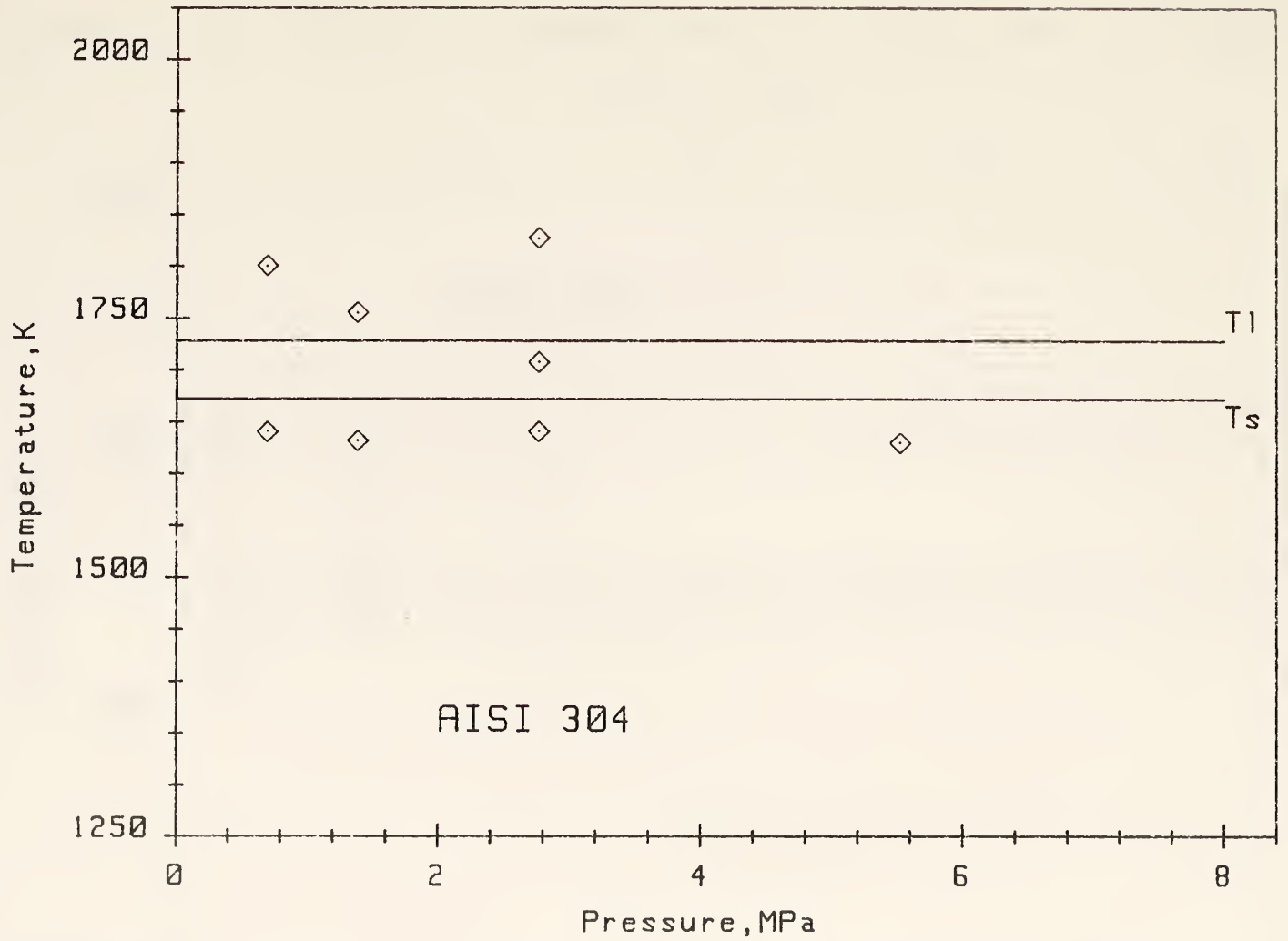


Figure 26. Average surface temperature at combustion for AISI 304.

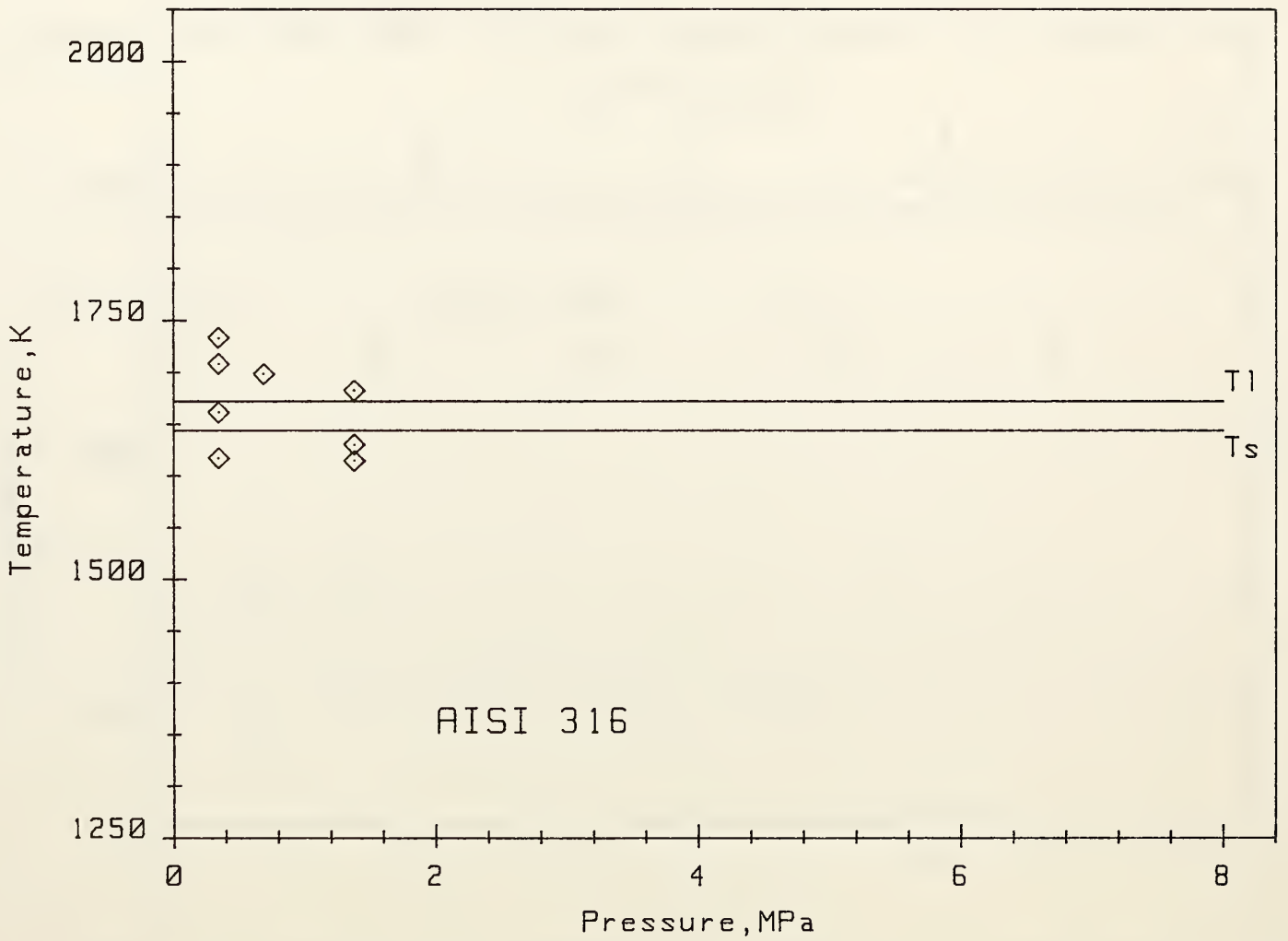


Figure 27. Interior temperature at ignition for AISI 316.

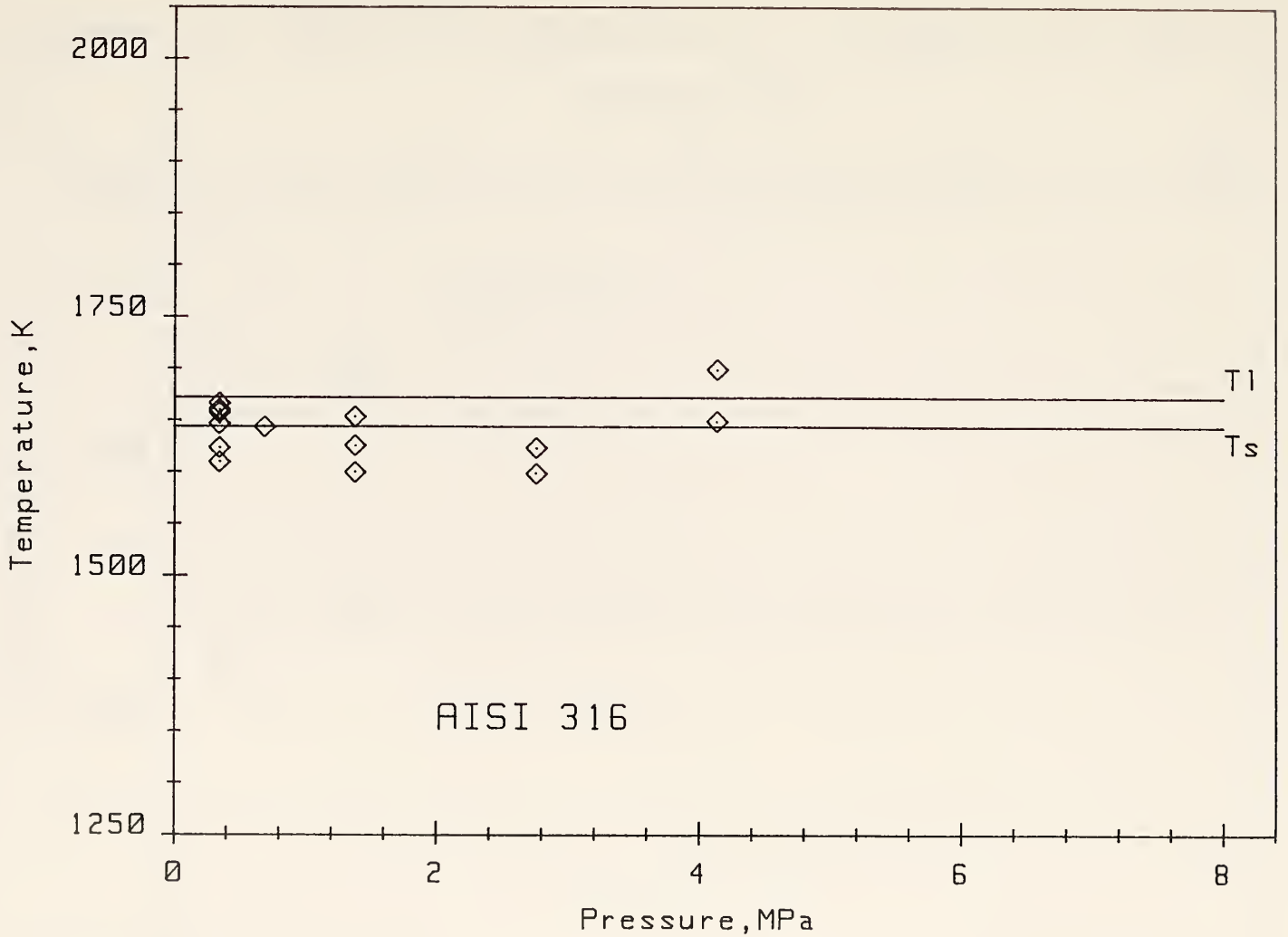


Figure 28. Average surface temperature at ignition for AISI 316.

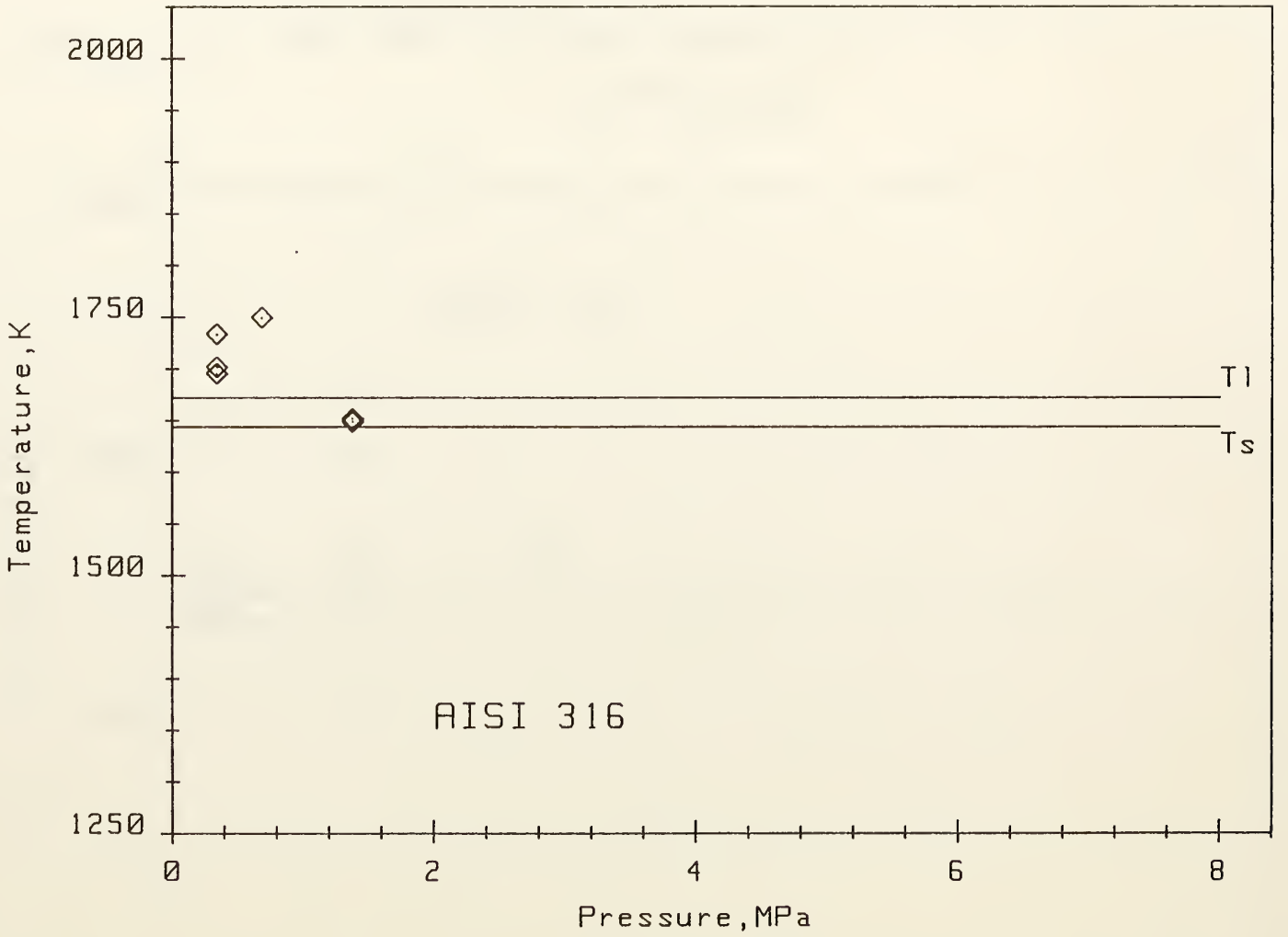


Figure 29. Interior temperature at combustion for AISI 316.

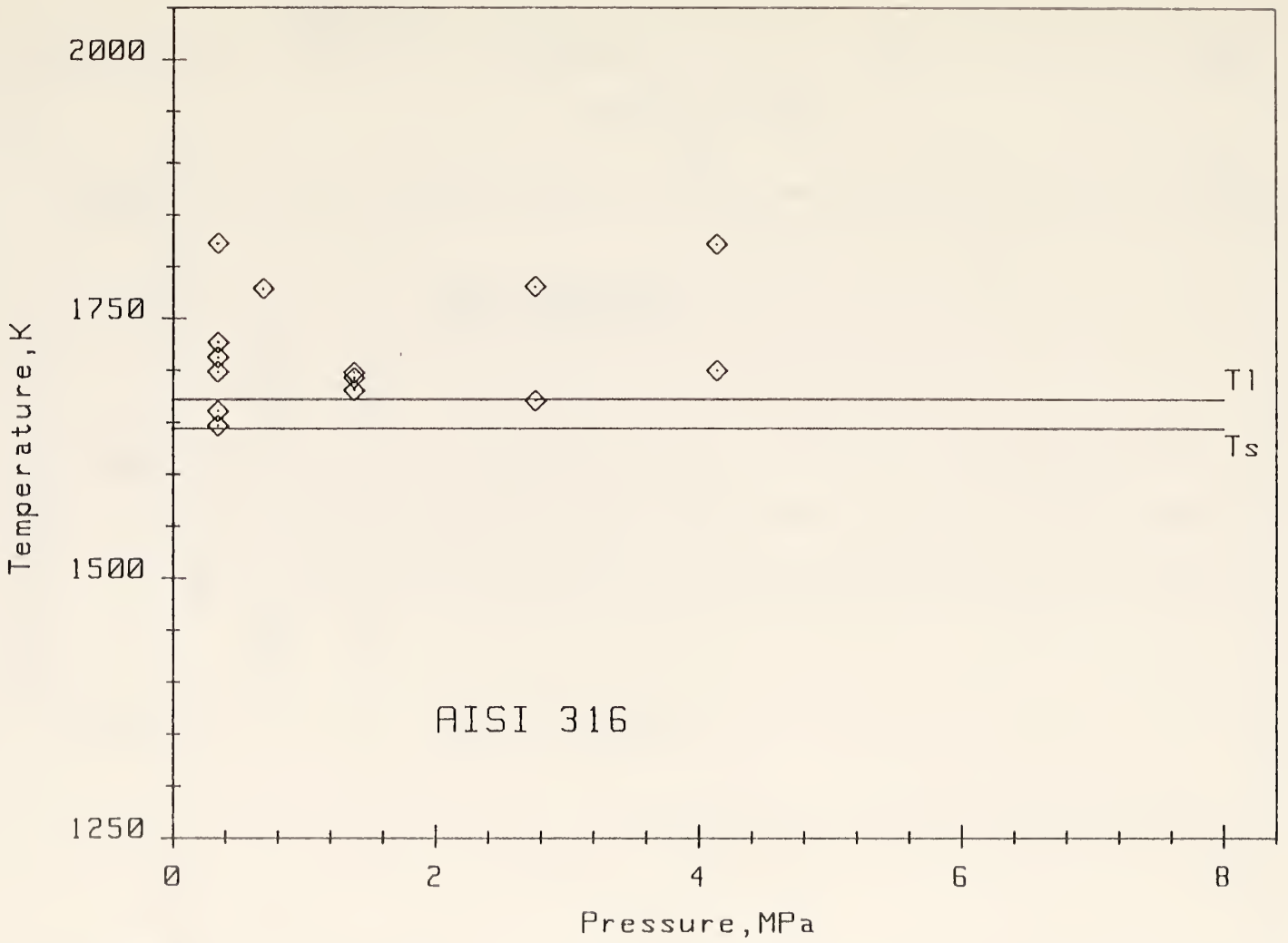


Figure 30. Average surface temperature at combustion for AISI 316.

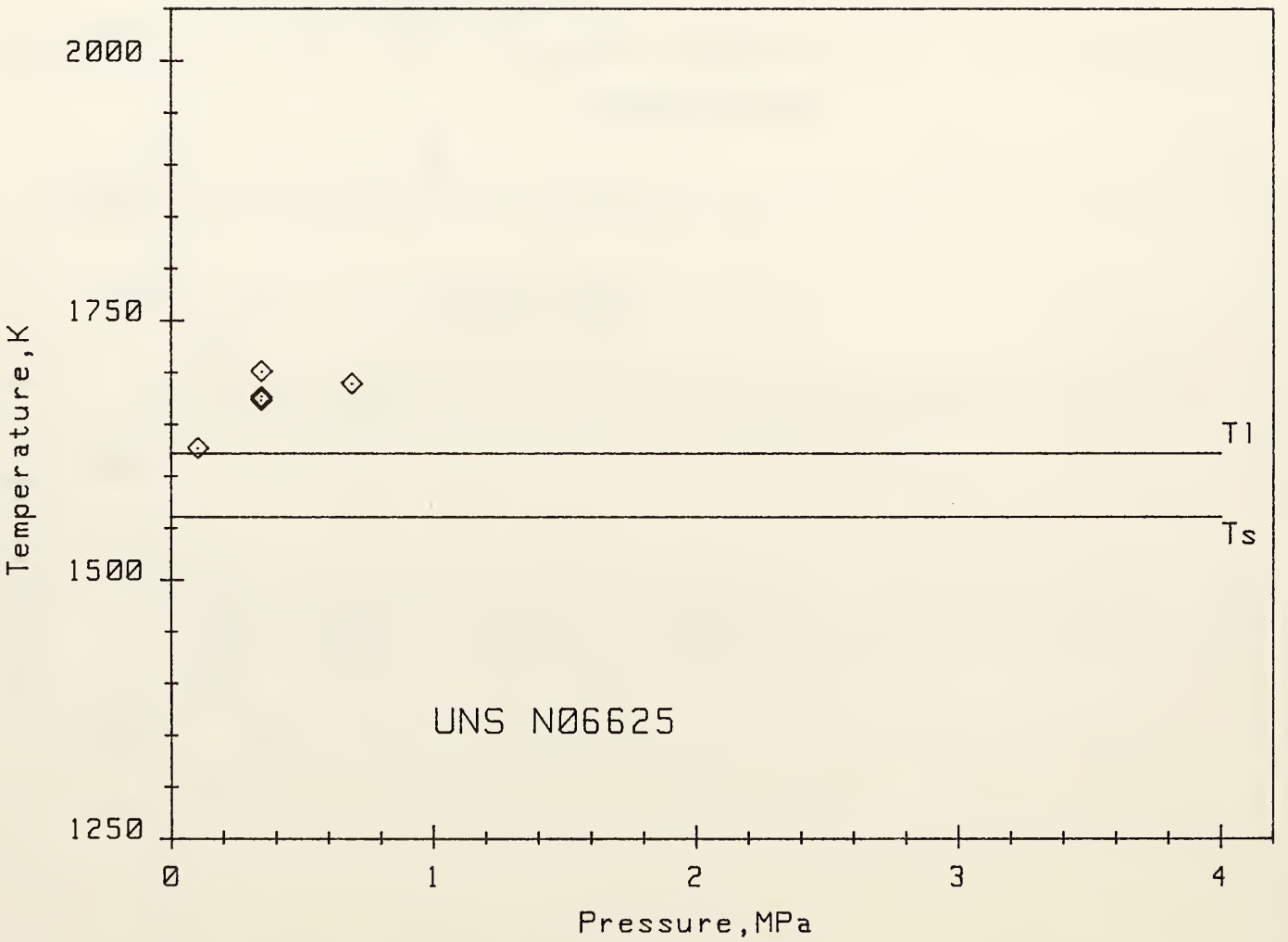


Figure 31. Interior temperature at ignition for UNS N06625.

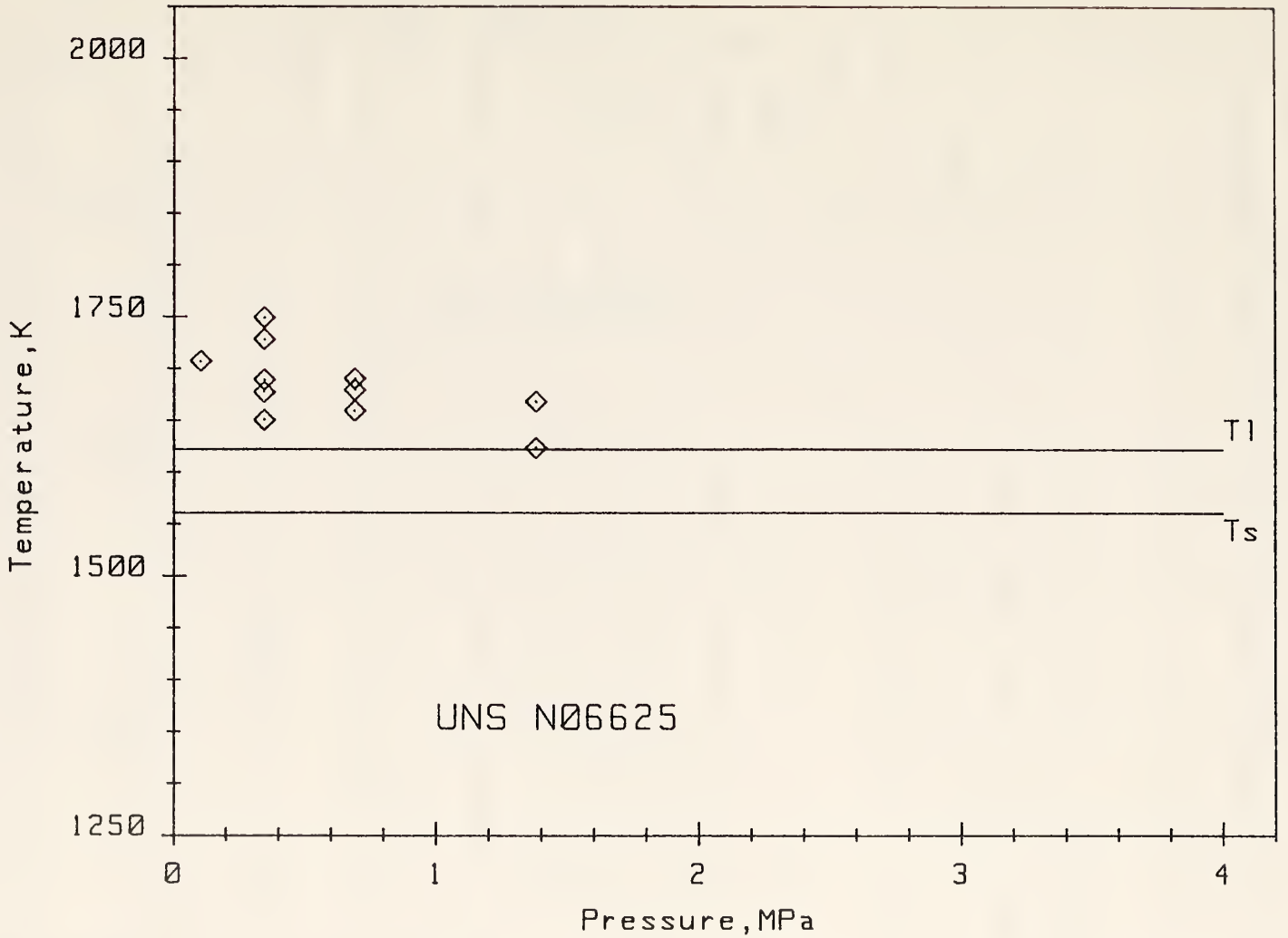


Figure 32. Average surface temperature at ignition for UNS N06625.

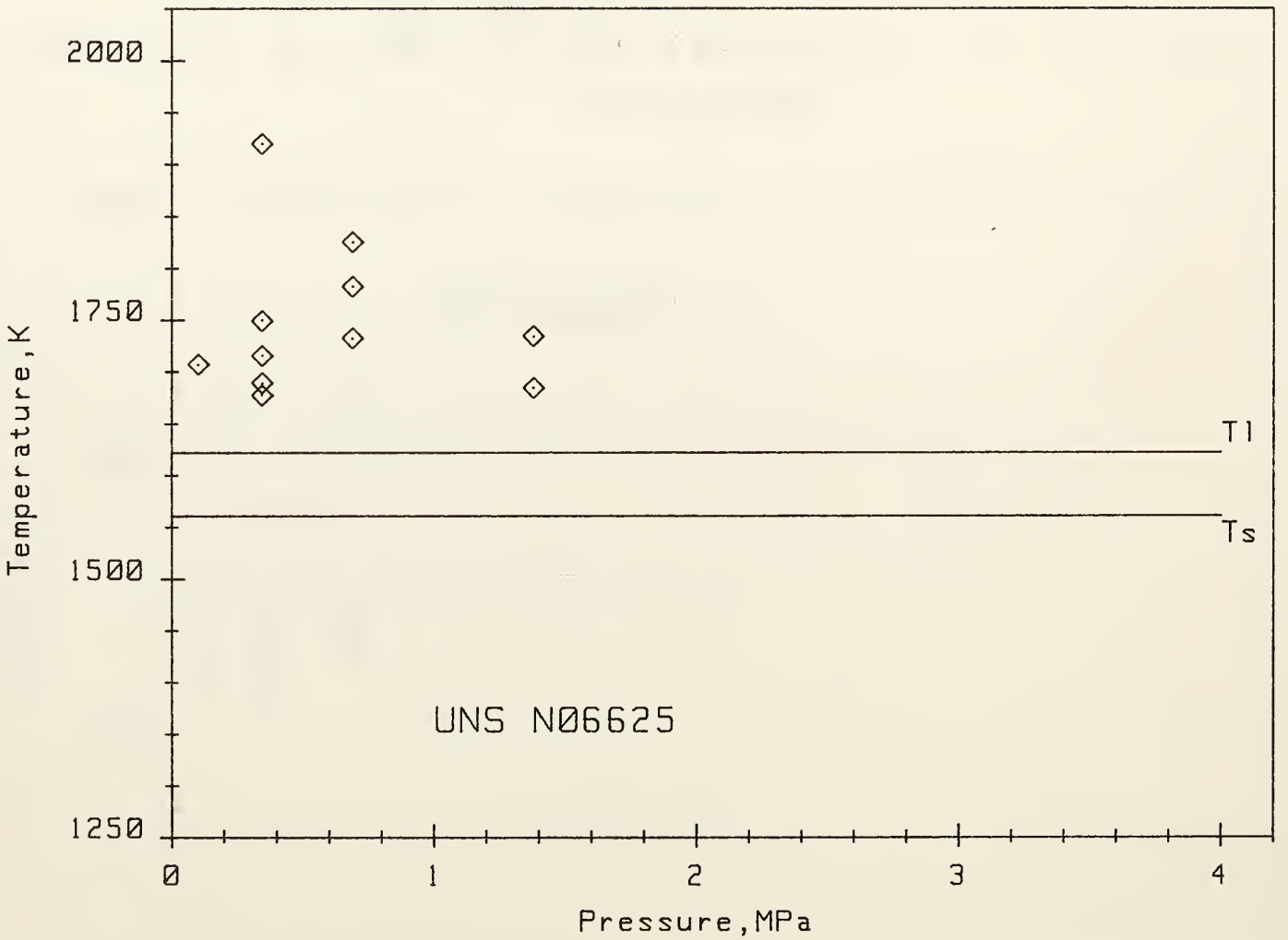


Figure 33. Average surface temperature at combustion for UNS N06625.

IV. SUMMARY AND FUTURE EFFORT

Several experimental problems have developed during the testing at elevated oxygen pressures. A summary of these difficulties and their resolution follow:

1. Insufficient laser power to reach ignition temperatures at high pressure. This difficulty has been resolved by acquiring a new 500 plus Watt laser.

2. Mass sensor disturbance by building vibrations. This difficulty is to be resolved by mounting the pressure chamber on a vibration damped table.

3. Mass sensor disturbance by convection currents. This difficulty has been partially resolved by restricting the area above the sample. However, additional work must be done.

4. Premature failure of the sample thermocouple. This difficulty was resolved by changing materials. However, the new material cannot be used beyond 2040 K. Therefore, interior temperature measurements on aluminum alloys cannot be made if ignition exceeds this temperature limit.

The acquisition of the new laser will ease the experimental problems. This unit can be computer controlled; thus heating rates can be programmed and maintained. Also, there is sufficient power to allow an increase in specimen size and to allow the sample to be "bathed" in the laser beam, allowing a more uniform surface temperature.

It has been found that aluminum alloys can be ignited at temperatures below the melting point of the surface oxide layer, in some cases, at temperatures significantly below. For these alloys, ignition and combustion are concurrent or almost so.

For the cobalt, iron, and nickel alloys, it has been found that unsupported combustion can only take place in the fluid state. Iron alloys can be ignited at temperatures slightly below the lower bounds of the melting range while cobalt

and nickel alloys can be ignited only when a fluid phase is present. To date, the ignition temperatures have no large oxygen pressure dependence.

Present plans call for bringing the new laser online under computer control. Programmed heating rates will be implemented and data will be generated for the present set of materials to the 13.8 MPa (2000 psia) pressure level, the maximum pressure that can be attained without pumps.

V. ACKNOWLEDGMENTS

The author would like to express his gratitude to Mr. James D. Breuel, Mr. James A. Hurley, and Mr. Ke Nguyen for their assistance in this study, and to the George C. Marshall Space Flight Center, Mr. John G. Austin, Jr., technical representative, for supporting this program.

APPENDIX A: Theory of Two-Color Ratio Pyrometry

Two color ratio pyrometry is a straightforward procedure which has one very strong feature: attenuation of the radiation, within reasonable limits, does not affect the temperature measurement. The theory of the method is described as follows for a unit wavelength interval.

Starting with the Planck equation for the spectral radiation, $W_B(\lambda)$, for a blackbody surface

$$W_B(\lambda) = 2 \pi c^2 h \lambda^{-5} (\exp(hc/\lambda kT-1)^{-1} \ [W/m^3], \qquad (A-1)$$

apply the Wien approximation

$$\exp(hc/\lambda kT) - 1 \approx \exp(hc/\lambda kT)$$

for $\lambda << hc/kT$

and obtain

$$W_B(\lambda) = 2 \pi c^2 h \lambda^{-5} \exp(-hc/\lambda kT) \ [W/m^3] \qquad (A-2)$$

where c = velocity of light in vacuum, m/s

h = Planck's constant, J·s

λ = wavelength of light, m

k = Boltzman's constant, J/k

T = absolute temperature, K.

The constants may be grouped and the blackbody spectral radiant emittance converted to graybody by

$$W(\lambda) = \varepsilon(\lambda) W_B(\lambda) = c_1 \varepsilon(\lambda) \lambda^{-5} \exp(-c_2/\lambda T) \qquad (A-3)$$

where

c_1 (first radiation constant) = $2 \pi h c^2$

c_2 (second radiation constant) = hc/k

and $\varepsilon(\lambda)$ is the spectral emissivity.

A ratio of the spectral radiant emittance at two wavelengths may now be defined:

$$R = W(\lambda_1)/W(\lambda_2) = \frac{\varepsilon(\lambda_1)}{\varepsilon(\lambda_2)} \cdot \frac{\lambda_2^5}{\lambda_1^5} \cdot \exp\left(\frac{c_2}{T}\left(\frac{1}{\lambda_1} - \frac{1}{\lambda_2}\right)\right). \qquad \text{(A-4)}$$

Taking the logarithm of the ratio and grouping constants obtain

$$\ell n\, R = \ell n \frac{\varepsilon(\lambda_1)}{\varepsilon(\lambda_2)} + 5\, \ell n \frac{\lambda_2}{\lambda_1} + \frac{c_2}{T}\left(\frac{1}{\lambda_1} - \frac{1}{\lambda_2}\right)$$

$$= A_1/T + A_0 + \ell n \frac{(\lambda_1)}{(\lambda_2)} \text{ where} \qquad \text{(A-5)}$$

$$A_0 = 5/n \frac{\lambda_2}{\lambda_1} \quad \text{and} \quad A_1 = C_2\left(\frac{1}{\lambda_1} - \frac{1}{\lambda_2}\right)$$

The wavelengths chosen for the ratio computation must be such that $\varepsilon(\lambda_1) = \varepsilon(\lambda_2)$ (or nearly so); otherwise an emissivity correction would have to be applied.

To expand the argument to a radiation detector signal it need only be observed that the detector signal is directly proportional to the radiation intensity

$$S \propto W(\lambda) \qquad \text{or} \qquad S = K\, W(\lambda)$$

thus

$$R = W(\lambda_1)/W(\lambda_2) = S_1/S_2 \qquad \text{(A-6)}$$

The argument presented herein is for a unit wavelength. To expand the argument to a wavelength band complicates the development considerably and is best approached by numerical methods. To implement the numerical development, a detector, optical system, and wavelength band are defined and the detector signal calculated from

$$S = G\,\tau \int_{\lambda_1}^{\lambda_2} \varepsilon(\lambda)\, R(\lambda)\, F(\lambda)\, W(\lambda,T)\, d\lambda \qquad \text{(A-7)}$$

where: G - geometric factor

τ - optical transmission factor

$R(\lambda)$ - absolute responsivity of the detector

$F(\lambda)$ - filter transmission function

$\varepsilon(\lambda), W(\lambda)$ - are as previously defined.

$\text{Ln } R = \text{Ln } (S_1/S_2)$ may then be calculated from the Planck (or Wien approximation) radiation equation. It can then be seen that this result is linear with respect to $1/T$.

APPENDIX B: Data Definitions

The definition of terminology to accurately describe an event or events in an experiment which has widely varying and interacting phenomena is usually difficult; this study is no exception. A theoretical definition of ignition can be fairly easily defined. However, to extract this point from the experimental data in which multiple events take place is far from easy and straightforward except for the vapor burning materials. The definition of ignition and combustion point, as determined from the experimental data, for vapor burning and liquid burning materials is discussed below.

1. Vapor Burning Materials

The materials of the vapor burning type of interest to this program are aluminum and its alloys. Figures B.1 shows an expanded view of the ignition sequence of aluminum 6061 in 0.69 MPa (100 psia) oxygen. Data were taken at 20 ms intervals. The upper curve was the average surface temperature of the specimen, and the bottom curve was the mass. An ignition event is considered to be developing when a temperature increase breaks from the general average surface temperature trend. The ignition point is the last data point--or projected data point--before this trend break. For the data in Figure B.1, the trend break occurs at 20.12 s, and the major temperature step was at 20.16 s. This short interval between the trend break and the major temperature step is typical of an aluminum alloy ignition. Because of the typically short time between ignition development and full combustion, ignition and combustion are considered to be concurrent for this report and the ignition value is used. For the case shown, the average surface temperature at the ignition time of 20.12 s is 2101 K.

2. Liquid Burning Materials

The cobalt, iron, and nickel based metal alloys burn in the liquid phase. Figure B.2 shows an overall view of the average surface temperature of a

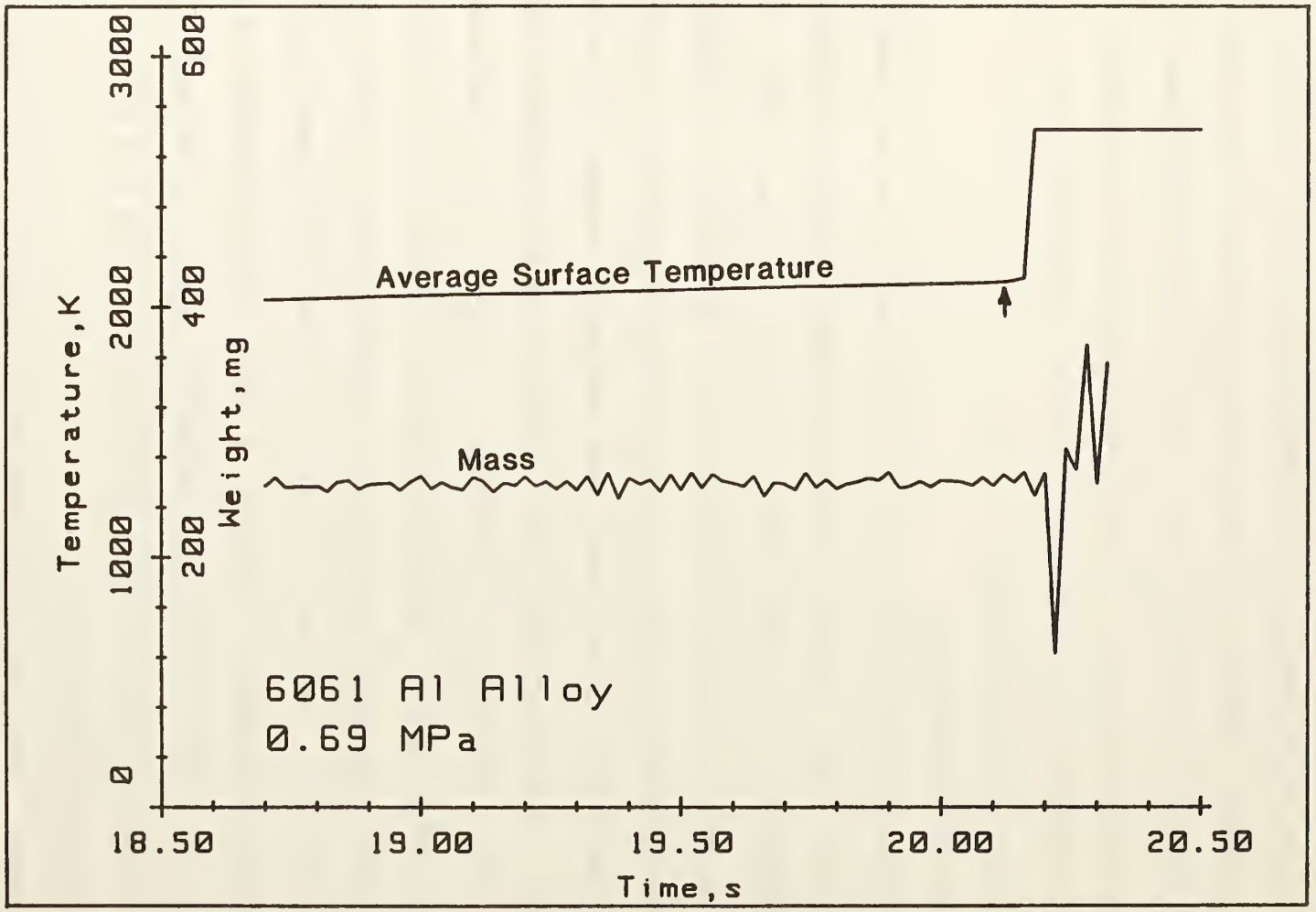


Figure B.1. Expanded view of an aluminum alloy ignition.

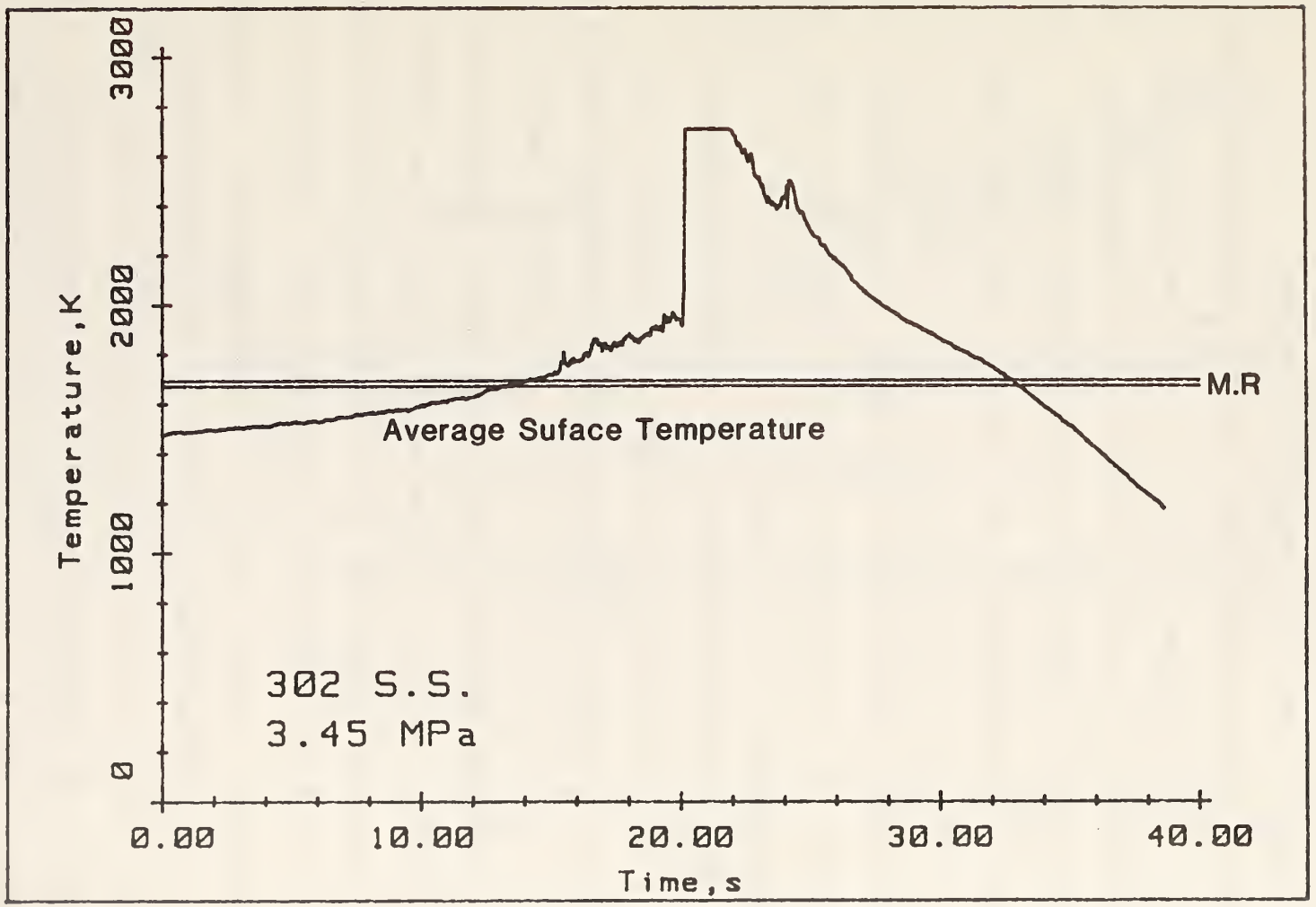


Figure B.2. Average surface temperature history for a test of a 300 series stainless steel.

test of a 300 series stainless steel. Figure B.3 is an expanded view of the ignition sequence of this same test. It must be pointed out that this example has been chosen to clearly illustrate the technique in determining the ignition and combustion points and is not typical of all test results.

The ignition sequence usually begins with the development of an ignition zone (hot-spot). This development occurs within the temperature region just prior to the beginning of the melting range to past the melting range. Thus, the waveforms of the data are complicated by phase and geometry changes. In addition to these changes, the oxide layer has built up to a significant thickness and may have a scaly or irregular surface texture which can give momentary hot-spots. These hot-spots appear to be an ignition zone on the surface temperature waveforms but are not. For a true ignition zone to be established, a small amount of material must be consumed. This can usually be detected on the mass waveform as well as the interior temperature waveform. The beginning development of the ignition zone is shown in Figure B.3 by the first set of markers at 15.28 s. The interior temperature response is delayed because the thermocouple interior position is a short distance from the ignition zone. To obtain a numerical value for the ignition temperature--interior, spot, average, etc.--a data point may be used or an extrapolating or averaging technique may be employed. The combustion point is found by determining the beginning time of an accelerating surface temperature trend ending in an almost instantaneous temperature step. In many cases the temperature accelerating time occurs for only a few data acquisition time periods. In other cases, the surface temperature acceleration occurs over several seconds and occasionally longer. As can be seen from Figure B.3, the existence of numerous hot-spots can mask the determination of the combustion point. However, for the example in Figure B.3, the combustion point is straightforward and occurs at 20.06 s. As in the case of the ignition temperature, the combustion

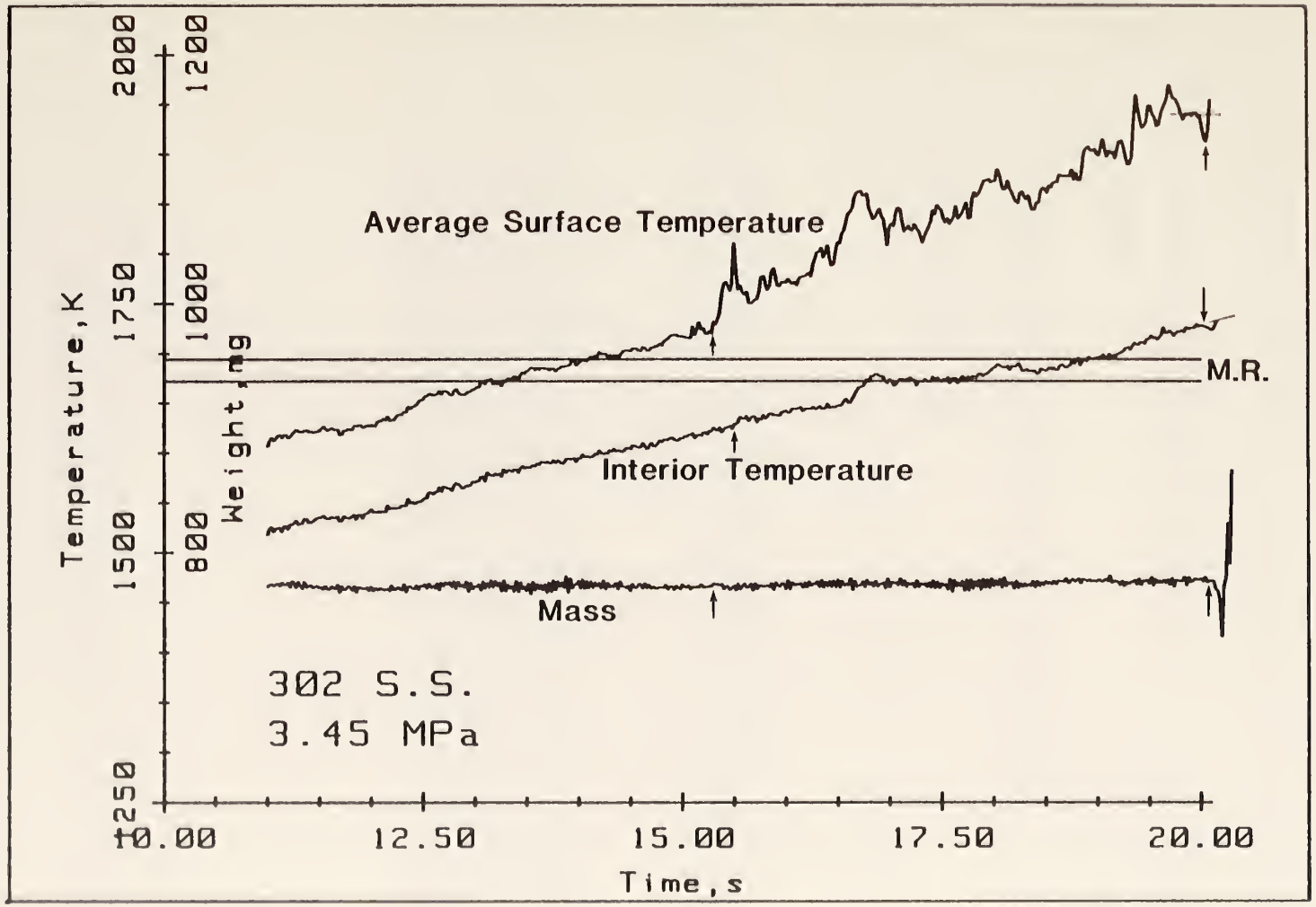


Figure B.3. Expanded view of the ignition and combustion sequence for a 300 series stainless steel.

temperature may be an individual data point or an averaged or extrapolated value. Occasionally the ignition point and the combustion point may be considered to be concurrent.

NBS-114A (REV. 2-8C)

U.S. DEPT. OF COMM. BIBLIOGRAPHIC DATA SHEET (See instructions)	1. PUBLICATION OR REPORT NO. NBSIR 84-3013	2. Performing Organ. Report No.	3. Publication Date August 1984

4. TITLE AND SUBTITLE

Laser-Initiated Combustion Studies on Metallic Alloys in Pressurized Oxygen

5. AUTHOR(S)

J. W. Bransford

6. PERFORMING ORGANIZATION (If joint or other than NBS, see instructions)

NATIONAL BUREAU OF STANDARDS
DEPARTMENT OF COMMERCE
WASHINGTON, D.C. 20234

7. Contract/Grant No.

8. Type of Report & Period Covered

9. SPONSORING ORGANIZATION NAME AND COMPLETE ADDRESS (Street, City, State, ZIP)

George C. Marshall Space Flight Center
Marshall Space Flight Center, Alabama

10. SUPPLEMENTARY NOTES

☐ Document describes a computer program; SF-185, FIPS Software Summary, is attached.

11. ABSTRACT (A 200-word or less factual summary of most significant information. If document includes a significant bibliography or literature survey, mention it here)

The interim results of ignition and combustion studies on aluminum, cobalt, iron, and nickel based alloys are presented. It was found that aluminum alloys could be ignited below the melting point of the product alloy oxides. It was also found that the cobalt, iron, and nickel based alloys generally ignited slightly below to slightly above the melting range of the respective alloy. Unsupported combustion could not be achieved until the alloys and oxides were in the liquid state.

12. KEY WORDS (Six to twelve entries; alphabetical order; capitalize only proper names; and separate key words by semicolons)

alloy; combustion; ignition; metal; oxygen compatibility

13. AVAILABILITY

☒ Unlimited

☐ For Official Distribution. Do Not Release to NTIS

☐ Order From Superintendent of Documents, U.S. Government Printing Office, Washington, D.C. 20402.

☒ Order From National Technical Information Service (NTIS), Springfield, VA. 22161

14. NO. OF PRINTED PAGES

76

15. Price

$10.00

*U.S. GOVERNMENT PRINTING OFFICE 1984-0-780-800/9451